Robust multi-response optimization considering location effect, dispersion effect, and model uncertainty using hybridization of NSGA-II and direct multi-search

An-Da Li[a,b], Zhen He[c], Yang Zhang[a,b,*]

[a] *School of Management, Tianjin University of Commerce, Tianjin 300134, China*
[b] *Management Innovation and Evaluation Research Center, Tianjin University of Commerce, Tianjin 300134, China*
[c] *College of Management and Economics, Tianjin University, Tianjin 300072, China*

Abstract

This paper proposes a robust method for multi-response optimization (MRO) considering the location effect, dispersion effect, and model uncertainty simultaneously. We propose a multi-objective optimization model for MRO that simultaneously maximizes the satisfaction degrees of the local and dispersion effects. Specifically, a robust desirability function is used to model the overall satisfaction degree of multiple responses with respect to the two effects. This desirability function evaluates a solution's performance considering the confidence intervals predicted by the regression models of location and dispersion effects, and thus, can address the problem of model uncertainty. The proposed multi-objective model yields a set of non-dominated solutions that approximate the Pareto front instead of one single solution, which provides more flexibility for decision makers to select the final best compromise solution based on their preferences. To solve the model, a hybrid multi-objective optimization algorithm called NSGAII-DMS that combines non-dominated sorting genetic algorithm II (NSGA-II) with direct multi-search (DMS) is proposed. NSGAII-DMS uses the search mechanism of NSGA-II during the early evolutionary phase to quickly find a set of non-dominated solutions and then uses the search mechanism of DMS to further tune the found non-dominated solutions. Two test examples have shown that the proposed multi-objective MRO model can produce a set of robust solutions by considering the location effect, dispersion effect, and model uncertainty. Further analyses illustrate that NSGAII-DMS shows significantly better search performance than several well-known multi-objective optimization algorithms, which include NSGA-II, SPEA2, MOEA/D, and DMS.

Keywords: Response surface methodology, Robust multi-response optimization, Model uncertainty, Desirability function approach, Multi-objective optimization

*Please cite this article as: Li, A.-D., He, Z., & Zhang, Y. (2022). Robust multi-response optimization considering location effect, dispersion effect, and model uncertainty using hybridization of NSGA-II and direct multi-search. Computers & Industrial Engineering, 169, 108247. https://doi.org/10.1016/j.cie.2022.108247

*Corresponding author
Email addresses: adli@tjcu.edu.cn (An-Da Li), zhhe@tju.edu.cn (Zhen He), yzhang@tjcu.edu.cn (Yang Zhang)

1. Introduction

Response surface methodology (RSM) is widely used for product quality and manufacturing process improvements (Box et al., 1987; Myers et al., 2016; Montgomery, 2017). It contains a set of statistical and optimization tools with respect to design of experiments (DOE), empirical model building, and optimization (Myers, 1999). RSM was first used for single response optimization (SRO) problems, which aims to find the optimal setting for input variables with respect to one single response variable (e.g., a quality variable). However, many products/processes in modern industries include multiple responses. For example, in the laser gyroscope manufacturing process of a company, the quality (response) variables include zero bias, bias stability, bias repeatability, etc. Therefore, it is required to simultaneously optimize the multiple responses by selecting the optimal setting for input variables. This optimization problem is called multi-response optimization (MRO) (Myers et al., 2016).

Since directly optimizing multiple responses is generally intractable, many creative approaches have been proposed to form MRO into a single objective optimization model. These approaches include the goal programming approach (Kazemzadeh et al., 2008), generalized distance approach (Khuri & Conlon, 1981), compromise programming approach (Costa et al., 2012a), probabilistic approach (Peterson et al., 2009), loss function approach (Taguchi, 1986; Pignatiello, 1993), and desirability function approach (Derringer, 1994). Except for the above studies, some studies (Lee et al., 2011; Chapman et al., 2014a,b; Costa & Lourenço, 2017; Ouyang et al., 2021) have applied multi-objective optimization algorithms for simultaneously optimizing multiple responses to find a set of non-dominated solutions instead of one single solution. However, one drawback of these methods is that it will be hard to optimize the defined MRO model if there are a large number of responses (more than three objectives).

To obtain a robust parameter setting for input variables in a response optimization problem, both the location and dispersion effects should be considered. The location effect denotes a response's bias compared with the target while the dispersion effect denotes the variance (i.e., robustness) of a response. The loss function approach (Taguchi, 1986; Pignatiello, 1993) can be applied to solve such a problem since both the location and dispersion effects can be measured by a loss function. Moreover, the dual-response methods (Vining & Myers, 1990; Kim & Lin, 1998; Zeybek et al., 2020) were proposed for robust response optimization. These methods model the location and dispersion effects as two separate "responses" to be optimized. Based on the idea of dual-response optimization, Kim & Lin (2006) proposed an MRO method that simultaneously optimizes the location and dispersion effects of multiple responses. The desirability function is adopted to obtain the degrees of satisfaction in terms of the means and standard deviations of the responses. The optimization model is then defined as maximizing the minimum degree of satisfaction over multiple responses.

The empirical response models established based on the experimental data depict the relations between

the input variables and the responses. In fact, the response models cannot be perfectly fitted, which leads to the problem of model uncertainty. Recently, some creative approaches have been proposed to handle the model uncertainty problem in MRO to obtain a more reliable solution. For example, Ko et al. (2005), Ouyang et al. (2017), and Feng et al. (2021) proposed several modified loss functions considering model uncertainty for MRO. Peterson et al. (2009), Wang et al. (2016, 2020), Ouyang et al. (2020, 2022), and Yang et al. (2021) proposed several Bayesian-based MRO methods. Since the Bayesian approach can obtain the posterior probability that a response falls into the defined tolerance interval, the model uncertainty problem is naturally handled. Another widely used strategy to address model uncertainty is considering a response's overall performance in the confidence interval instead of the mean response value predicted by the model. Xu & Albin (2003) proposed a min-max deviation model that considers every point in the confidence interval for a response to handle the uncertainty caused by model coefficients. Gülpınar & Rustem (2007) proposed a worst-case strategy that uses the worst response value predicted by the uncertain model for constructing the response optimization model. He et al. (2012) adopted the worst-case strategy to form a robust desirability function to build an MRO method. This method inherits the advantages of the traditional desirability function approach, whereas it neglects the dispersion effect. Based on the idea of the robust desirability function, He et al. (2017) proposed a robust fuzzy programming method that considers the location effect, dispersion effect, and model uncertainty. One limitation of this method is that it only considers the uncertainty of the location effect. It is beneficial to consider the uncertainty of the dispersion effect as well.

Most existing dual-response methods construct a single objective optimization model to optimize the location and dispersion effects. To form the optimization model, decision makers' (DMs') preferences are required to balance the priorities of the two effects, which is not an easy task because extensive domain knowledge is required. Recently, several multi-objective methods (Köksoy & Doganaksoy, 2003; Köksoy & Yalcinoz, 2008; Shin & Cho, 2009; Lee et al., 2009; Costa et al., 2012b) for robust response optimization were proposed to find a set of non-dominated solutions (i.e., parameter settings) by simultaneously optimizing the two effects. These methods do not proactively use the DMs' preferences during the optimization. In comparison, DMs can select the best compromise solution from the non-dominated solutions according to their preferences or by using multi-objective decision methods after the optimization. However, these multi-objective methods are limited since they can only handle the SRO problems. To address multiple responses, Lee et al. (2018) proposed a multi-objective MRO method based on the desirability function. This method separately models the overall degrees of satisfaction with respect to the location and dispersion effects of multiple responses. The two effects are then optimized by a multi-objective optimization algorithm and the posterior preference articulation approach is used to select the final solution. However, the drawback of this method is that model uncertainty is not considered.

As mentioned above, to obtain a robust parameter setting for MRO, it is required to consider the

location and dispersion effects of the responses, as well as model uncertainty. Moreover, a multi-objective optimization algorithm can return a set of non-dominated solutions with different combinations of the degrees of satisfaction with respect to the location and dispersion effects, which provides DMs with more flexibility to further select a desirable solution considering their preferences. Therefore, proposing a multi-objective optimization based MRO model that addresses both the location and dispersion effects while considering model uncertainty is required. To solve the response optimization problems, evolutionary algorithms, such as genetic algorithms (GAs) (Köksoy & Yalcinoz, 2008; Wang et al., 2016), are generally used due to their good global search performance. Non-dominated sorting genetic algorithm II (NSGA-II) (Deb et al., 2002) is one of the most popular multi-objective evolutionary algorithms (MOEAs) that can find a set of non-dominated solutions approximating the true Pareto front by simultaneously optimizing multiple objective functions, and thus can be used to solve the constructed MRO model. NSGA-II can search in a large solution space with the population-based solution updating strategy, which endows it with a good global search ability. However, being a type of GA, NSGA-II is weak in fine-tuning solutions when they are very close to optimal solutions because the genetic operators in GAs introduce too much randomness (Oh et al., 2004). He et al. (2012) proposed a hybrid algorithm combining a GA with a direct search (also known as pattern search) algorithm to rectify the mentioned weakness of the GAs. The hybrid algorithm first adopts the GA to optimize the established desirability function for MRO, and then uses the direct search algorithm for further optimization. However, this hybrid algorithm is proposed for a single optimization model, and thus, it does not apply to multi-objective MRO models. Therefore, it would be beneficial to propose an effective multi-objective optimization algorithm that combines NSGA-II with a direct search algorithm for the MRO model. To narrow the above stated research gaps, this paper proposes a novel multi-objective optimization based MRO method, which includes a multi-objective MRO model and a multi-objective optimization algorithm. The main contributions of this paper are summarized as follows:

- We construct the MRO problem as a multi-objective optimization model that maximizes the desirability values of both the location and dispersion effects. To address model uncertainty, we adopt the idea of robust desirability function (He et al., 2012) and construct two desirability functions that model the overall location and dispersion effects of multiple responses, respectively.

- We propose a hybrid optimization algorithm called NSGAII-DMS that combines NSGA-II with direct multi-search (DMS) (Custódio et al., 2011), a recently proposed multi-objective optimization algorithm based on the direct search, to solve the constructed multi-objective MRO model. In the proposed optimization algorithm, NSGA-II is used first to find a set of non-dominated solutions, and then, DMS is used to further update the non-dominated solutions by searching in the local area around the solutions found by NSGA-II.

- We show the effectiveness of the constructed MRO model with two test examples and verify the

performance of NSGAII-DMS by comparing it with several well-known multi-objective optimization algorithms.

- We propose to use the ideal point method (IPM) Li et al. (2016) to help DMs to select the best compromise solution from the non-dominated solutions found by NSGAII-DMS. The results of the test examples show that IPM is a desirable tool for decision making.

The remainder of this paper is organized as follows. Section 2 presents the preliminaries, which are basic concepts for the proposed method. Section 3 describes the details of the proposed MRO model. Section 4 introduces the proposed NSGAII-DMS algorithm. Section 5 evaluates the performance of the proposed MRO model with two test examples. Section 6 verifies the search performance of the proposed optimization algorithm NSGAII-DMS. The conclusions and future research interests are given in Section 7.

2. Preliminaries

This section presents the basic concepts for the proposed method, including a brief introduction of the multi-objective optimization problems (MOPs) and a brief introduction of the desirability function based MRO methods.

2.1. Multi-objective optimization problems

An MOP aims to simultaneously minimize/maximize multiple objective functions. The mathematical formula of an MOP with m objectives can be written as

$$\begin{aligned} \text{minimize} \quad & \mathbf{F}(\mathbf{x}) = [f_1(\mathbf{x}), f_2(\mathbf{x}), ..., f_m(\mathbf{x})]^T \\ \text{subject to} \quad & \mathbf{x} \in \mathbb{X} \end{aligned}, \tag{1}$$

where $\mathbf{x} = [x_1, x_2, ..., x_n]^T \in \mathbb{R}^n$ is a vector (solution) of n decision variables, $f_j(\mathbf{x})$ $(j = 1, 2, ..., m)$ denotes the jth objective function, and $\mathbb{X}$ denotes the set of all feasible solutions. In MOPs, a solution's goodness is determined by the trade-offs among the objectives. Given two solutions $\mathbf{x}_1$ and $\mathbf{x}_2$ for the problem in Eq. (1), $\mathbf{x}_1$ is better than $\mathbf{x}_2$ if

$$\forall j : f_j(\mathbf{x}_1) \leq f_j(\mathbf{x}_2) \quad \text{and} \quad \exists j : f_j(\mathbf{x}_1) < f_j(\mathbf{x}_2). \tag{2}$$

We say that $\mathbf{x}_1$ dominates $\mathbf{x}_2$ (denoted by $\mathbf{x}_1 \prec \mathbf{x}_2$) if $\mathbf{x}_1$ is better than $\mathbf{x}_2$. If a solution $\mathbf{x}^*$ is not dominated by any feasible solution $\mathbf{x} \in \mathbb{X}$, $\mathbf{x}^*$ is said to be a Pareto optimal solution. Generally, an MOP has a set of Pareto optimal solutions. The surface formed by the Pareto optimal solutions in the objective space is called the Pareto front. The objective of a multi-objective optimization algorithm is to find a set of well distributed non-dominated solutions approximating the true Pareto front.

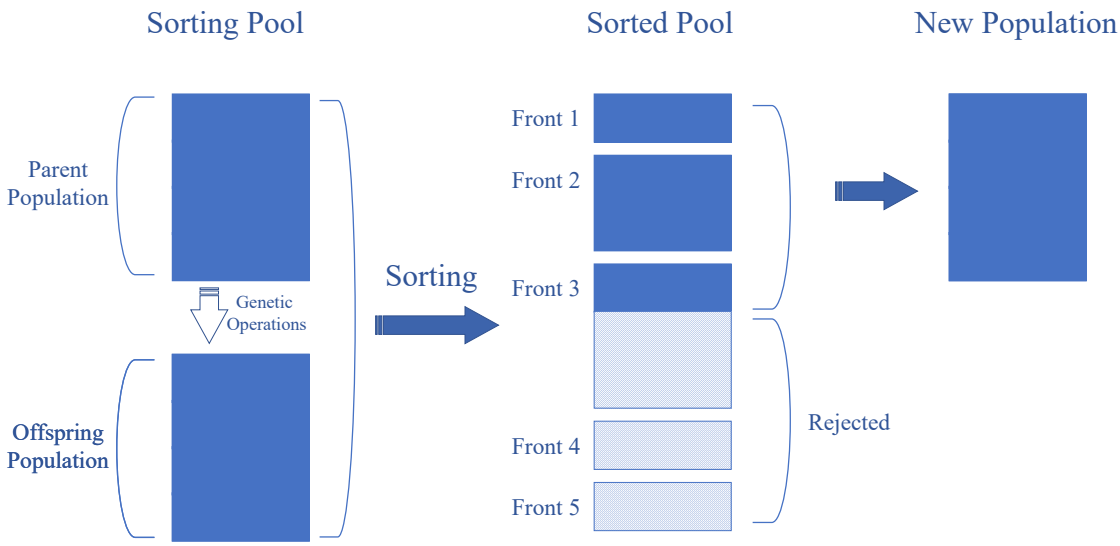

Figure 1: Illustration of the procedure of NSGA-II at a generation.

2.2. NSGA-II

In recent years, many MOEAs have been proposed to solve MOPs. These algorithms can obtain a set of non-dominated solutions approximating the true Pareto front. MOEAs have the advantages of being derivative-free, good global search performance, easy implementation, etc. Thus, they can be easily applied to various MOPs. NSGA-II is one of the most popular MOEAs proposed by Deb et al. (2002). We briefly introduce the idea of NSGA-II as follows.

Fig. 1 illustrates the procedure of NSGA-II at a generation. Suppose that the population has N solutions. At each generation, the offspring population with N solutions is produced by the genetic operators based on the parent population. A sorting pool is generated by combining the parent and offspring populations. The fast non-dominated sorting approach and crowding distance measure are used then to sort the solutions in the sorting pool. The best N solutions in the sorted pool are added to the new population for the next generation. Specifically, the fast non-dominated sorting approach can divide the solutions in the sorting pool into several non-dominated fronts (5 in the example shown in Fig. 1) according to the Pareto dominance concept, where a lower front level denotes a better fitness level of the solution. To compare the solutions within the same non-dominated front, the crowding distance that measures the density of solutions around a particular solution is used in NSGA-II. A solution with a larger crowding distance is said to have a better fitness level. Using the fast non-dominated sorting approach and crowding distance measure simultaneously, any two solutions in the sorting pool can be compared, which is beneficial for sorting the solutions with respect to their goodness.

2.3. Direct multi-search (DMS)

DMS is a recently proposed multi-objective optimization algorithm based on the idea of direct search (Custódio et al., 2011). It mainly adopts a search mechanism named *poll step* to update solutions during the optimization process. DMS has shown to have excellent convergence behaviors for continuous MOPs, and thus, can be used for solving the established multi-objective MRO model in this paper.

The poll step of DMS at an iteration can be briefly introduced as follows. Let $\mathbf{x}_p$ be a poll center selected from the set (denoted by L_{ns}) of non-dominated solutions found so far. Then, a set L_{trial} of new solutions is generated as

$$L_{trial} = \{\mathbf{x}_p + \alpha_{\mathbf{x}_p}\mathbf{d} | \mathbf{d} \in D\} \tag{3}$$

where D is a randomly generated positive spanning set at this iteration, $\mathbf{d}$ is a vector in D that decides a search direction, $\alpha_{\mathbf{x}_p}$ is a step size parameter of $\mathbf{x}_p$ that decides the length of the search. The generated solutions in L_{trial} can be then used to update the non-dominated set L_{ns} based on the Pareto dominance concept. We say that the poll step succeeds if L_n is successfully updated, and otherwise, we say the poll step fails. The step size parameter of the poll center is updated to $\alpha_{\mathbf{x}_p,new} \geq \alpha_{\mathbf{x}_p}$ if the poll step succeeds, and is updated to $\alpha_{\mathbf{x}_p,new} < \alpha_{\mathbf{x}_p}$ if the poll step fails. It indicates that DMS can gradually reduces the search space when the poll step fails, which results in good local search performance and excellent convergence behaviors. Each new generated solution $\mathbf{x}_t \in L_{trial}$ has a step size parameter $\alpha_{\mathbf{x}_t}$ as well, which inherits the value of $\alpha_{\mathbf{x}_p}$, i.e., $\alpha_{\mathbf{x}_t} = \alpha_{\mathbf{x}_{p,new}}$.

2.4. MRO methods using desirability functions

Let $\mathbf{x} = [x_1, x_2, ..., x_n]^T$ be a vector of n input variables and y be a response variable. An RSM method generally uses a quadratic model to depict the relation between $\mathbf{x}$ and y as

$$y(\mathbf{x}) = \beta_0 + \sum_{i=1}^{n} \beta_i x_i + \sum_{i=1}^{n} \beta_{ii} x_i^2 + \sum_{i<j} \sum_{j=2}^{n} \beta_{ij} x_i x_j + \epsilon, \tag{4}$$

where $\epsilon \sim N(0, \sigma^2)$ is the experimental error term. Let

$$\mathbf{z}(\mathbf{x}) = [1, x_1, ..., x_n, x_1^2, ..., x_n^2, x_1x_2, ..., x_{n-1}x_n]^T \tag{5}$$

and

$$\boldsymbol{\beta} = [\beta_0, \beta_1, ..., \beta_n, \beta_{11}, ..., \beta_{nn}, \beta_{12}, ..., \beta_{n-1,n}]^T. \tag{6}$$

The model in Eq.(4) can be depicted as

$$y(x) = \mathbf{z}(\mathbf{x})^T \boldsymbol{\beta} + \epsilon. \tag{7}$$

Suppose that g samples are obtained in the experiment, $\mathbf{X}$ is a $g \times n$ matrix denoting the observations of $\mathbf{x}$, and $\mathbf{y}$ is a $g \times 1$ vector denoting the observations of the response y. Using the least squares estimation, the vector of estimated parameters is obtained as $\hat{\boldsymbol{\beta}} = (\mathbf{X}^T\mathbf{X})^{-1}\mathbf{X}^T\mathbf{y}$, and the estimated response value is obtained as $\hat{y}(\mathbf{x}) = \mathbf{z}(\mathbf{x})^T\hat{\boldsymbol{\beta}}$. Under the assumption that the experimental errors are independently identically distributed, the standard error of the predicted response is obtained as

$$Se[\hat{y}(\mathbf{x})] = \sqrt{\hat{\sigma}^2\mathbf{z}(\mathbf{x})^T(\mathbf{X}^T\mathbf{X})^{-1}\mathbf{z}(\mathbf{x})}. \tag{8}$$

Then, the $(1-\alpha)$ confidence interval $[y^L(\mathbf{x}), y^U(\mathbf{x})]$ of the true response $y(\mathbf{x})$ is obtained as

$$[y^L(\mathbf{x}), y^U(\mathbf{x})] = [\hat{y}(\mathbf{x}) - t_{\alpha/2,g-p} \cdot Se[\hat{y}(\mathbf{x})], \hat{y}(x) + t_{\alpha/2,g-p} \cdot Se[\hat{y}(x)]] \tag{9}$$

where $t_{\alpha/2,g-p}$ is the $1-\alpha/2$ quantile of a Student's t-distribution with $g-p$ degrees of freedom, g is the number of samples obtained in the experiment, and p is the number of estimated parameters.

In an MRO problem with m independent responses y_j $(j = 1, ..., m)$, we can use the aforementioned model to obtain the estimated response value $\hat{y}_j(\mathbf{x})$, standard error $Se[\hat{y}_j(\mathbf{x})]$, and the confidence interval $[y_j^L(\mathbf{x}), y_j^U(\mathbf{x})]$ for each response. The desirability function approach introduced by Derringer (1994) is a very popular and powerful technique that can comprehensively evaluate the overall degree of satisfaction of multiple responses. This approach first transforms each predicted $\hat{y}_j(\mathbf{x})$ into a desirability value $d(\hat{y}_j(\mathbf{x})) \in [0, 1]$ (larger is better), which reflects the degree of satisfaction of each response with respect to the target. Then, the overall desirability value of all responses is calculated using the function

$$D(\mathbf{x}) = \Big(\prod_{j=1}^{m} d(\hat{y}_j(\mathbf{x}))^{w_j}\Big)^{1/\sum w_j} \tag{10}$$

where $w_j > 0$ denotes the weight of response y_j. Finally, the MRO problem is defined as an optimization model that maximizes the overall desirability function $D(\mathbf{x})$.

The drawback of Derringer's method is that it neglects the fact that the predicted responses $\hat{y}_j(\mathbf{x})$ $(j = 1, ..., m)$ are unreliable to some extent due to the uncertainty of the fitted regression models. In other words, this method does not consider the problem of model uncertainty. Recently, He et al. (2012) proposed a robust desirability function that considered model uncertainty in modeling the overall desirability degree of multiple responses. Specifically, a response's desirability level is measured by the worst desirability value produced by the confidence interval $[y_j^L(\mathbf{x}), y_j^U(\mathbf{x})]$, and it is obtained as

$$d_j^r(\mathbf{x}) = \min\{d(y_j^L(\mathbf{x})), d(y_j^U(\mathbf{x}))\}. \tag{11}$$

Then, a robust overall desirability value for multiple responses can be obtained based on Eq. (10) by

replacing $d(\hat{y}_j(\mathbf{x}))$ with $d_j^r(\mathbf{x})$.

3. Proposed multi-objective optimization model for MRO

This section proposes a multi-objective optimization model that considers the location effect, dispersion effect, and model uncertainty simultaneously for MRO. Suppose that an MRO problem contains m independent responses. Using the quadratic model described in Section 2.4, we can get the predicted mean (location effect) $\hat{y}_{j,\mu}(\mathbf{x})$ $(j = 1, ..., m)$ and the predicted standard deviation (dispersion effect) $\hat{y}_{j,\sigma}(\mathbf{x})$ $(j = 1, ..., m)$ of each response. Moreover, the $1 - \alpha$ confidence intervals $[y_{j,\mu}^L(\mathbf{x}), y_{j,\mu}^U(\mathbf{x})]$ and $[y_{j,\sigma}^L(\mathbf{x}), y_{j,\sigma}^U(\mathbf{x})]$ for the mean and standard deviation of each response can be obtained by Eq. (9). Based on these notations, we model the overall location and dispersion effects of multiple responses based on the desirability function as follows.

3.1. Overall location effect considering model uncertainty

In this paper, we model the overall location effect of multiple responses with the desirability function approach. Specifically, the robust desirability function (He et al., 2012) that can handle the uncertainty of fitted models is used to model the overall location effect. The optimization objective for a response can be the nominal-the-best (NTB), the larger-the-better (LTB), or the smaller-the-better (STB) type. The desirability function for each of the three response types is shown as follows.

For an NTB type response y_j, the robust desirability function is defined as

$$d_{j,\mu}^r(\mathbf{x}) = \begin{cases} 0; & if \quad y_{j,\mu}^L(\mathbf{x}) \le y_{j,\mu}^{\min} \quad or \quad y_{j,\mu}^U(\mathbf{x}) \ge y_{j,\mu}^{\max} \\ \min\left\{ \left(\dfrac{y_{j,\mu}^L(\mathbf{x}) - y_{j,\mu}^{\min}}{T_{j,\mu} - y_{j,\mu}^{\min}} \right)^{s_j}, \left(\dfrac{y_{j,\mu}^{\max} - y_{j,\mu}^U(\mathbf{x})}{y_{j,\mu}^{\max} - T_{j,\mu}} \right)^{t_j} \right\}; & otherwise \end{cases} \tag{12}$$

where $y_{j,\mu}^{\min}$ and $y_{j,\mu}^{\max}$ denote the lower and upper specification limits of the response, respectively, $T_{j,\mu}$ denotes the target value of the response, and s_j and t_j are the parameters determining the shape of the desirability function (see Kim & Lin (1998) for more details). Specifically, $s_j = 1$ and $t_j = 1$ indicate a linear shape of the desirability function.

For an LTB type response y_j, the robust desirability function is defined as

$$d_{j,\mu}^r(\mathbf{x}) = \begin{cases} 0; & if \quad y_{j,\mu}^L(\mathbf{x}) \le y_{j,\mu}^{\min} \\ \left(\dfrac{y_{j,\mu}^L(\mathbf{x}) - y_{j,\mu}^{\min}}{T_{j,\mu} - y_{j,\mu}^{\min}} \right)^{t_j}; & if \quad y_{j,\mu}^{\min} < y_{j,\mu}^L(\mathbf{x}) < T_{j,\mu} \\ 1; & if \quad y_{j,\mu}^L(\mathbf{x}) \ge T_{j,\mu} \end{cases} \tag{13}$$

where $y_{j,\mu}^{\min}$ denotes the lower specification limit and $T_{j,\mu}$ denotes the target value of the response.

For an STB type response y_j, the robust desirability function is defined as

$$d^r_{j,\mu}(\mathbf{x}) = \begin{cases} 0; & if \quad y^U_{j,\mu}(\mathbf{x}) \geq y^{\max}_{j,\mu} \\ \left(\dfrac{y^{\max}_{j,\mu} - y^U_{j,\mu}(\mathbf{x})}{y^{\max}_{j,\mu} - T_{j,\mu}}\right)^{t_j}; & if \quad T_{j,\mu} < y^U_{j,\mu}(\mathbf{x}) < y^{\max}_{j,\mu} \\ 1; & if \quad y^U_{j,\mu}(\mathbf{x}) \leq T_{j,\mu} \end{cases} \tag{14}$$

where $y^{\max}_{j,\mu}$ denotes the upper specification limit and $T_{j,\mu}$ denotes the target value of response y_j. Using Eqs. (12)-(14), the robust desirability value $d^r_{j,\mu}(\mathbf{x})$ for each response can be obtained. Then, we can model the overall location effect of multiple responses with the robust overall desirability function

$$D^r_{\mu}(\mathbf{x}) = \Big(\prod_{j=1}^{m} d^r_{j,\mu}(\mathbf{x})^{w_{j,\mu}}\Big)^{1/\sum w_{j,\mu}}, \tag{15}$$

where $w_{j,\mu} > 0$ is the weight for the location effect of response y_j.

3.2. Overall dispersion effect considering model uncertainty

The robust desirability function method proposed by He et al. (2012) does not consider the dispersion effect of responses. In this paper, the dispersion effect of responses is considered as well. We model the overall dispersion effect in a similar way to the overall location effect. The dispersion effect $\hat{y}_{j,\sigma}(\mathbf{x})$ for a response y_j is always the STB type, and thus, it can be modeled considering model uncertainty as

$$d^r_{j,\sigma}(\mathbf{x}) = \begin{cases} 0; & if \quad y^U_{j,\sigma}(\mathbf{x}) \geq y^{\max}_{j,\sigma} \\ \left(\dfrac{y^{\max}_{j,\sigma} - y^U_{j,\sigma}(\mathbf{x})}{y^{\max}_{j,\sigma} - T_{j,\sigma}}\right)^{t_{j,\sigma}}; & if \quad T_{j,\sigma} < y^U_{j,\sigma}(\mathbf{x}) < y^{\max}_{j,\sigma} \\ 1; & if \quad y^U_{j,\sigma}(\mathbf{x}) \leq T_{j,\sigma} \end{cases}, \tag{16}$$

where $y^{\max}_{j,\sigma}$ and $T_{j,\sigma}$ denote the upper specification limit and the target value of the standard deviation of response y_j, and $t_{j,\sigma}$ defines the shape of the desirability function. Then, the overall location effect of multiple responses can be modeled by the overall robust desirability function

$$D^r_{\sigma}(\mathbf{x}) = \Big(\prod_{j=1}^{m} d^r_{i,\sigma}(\mathbf{x})^{w_{j,\sigma}}\Big)^{1/\sum w_{j,\sigma}}, \tag{17}$$

where $w_{j,\sigma} > 0$ is the weight for the dispersion effect of response y_j.

3.3. The optimization model

In this paper, we optimize the location and dispersion effects of multiple responses simultaneously. The overall location and dispersion effects of multiple responses can be modeled by the robust desirability

functions in Eqs. (15) and (17), respectively. The desirability function values $D_{\mu}^{r}(\mathbf{x})$ and $D_{\sigma}^{r}(\mathbf{x})$ for the two effects are the larger the better. Therefore, we can formulate the optimization model as an MOP of maximizing both $D_{\mu}^{r}(\mathbf{x})$ and $D_{\sigma}^{r}(\mathbf{x})$. Seeing that the desirability function values $D_{\mu}^{r}(\mathbf{x})$ and $D_{\sigma}^{r}(\mathbf{x})$ are in $[0,1]$ according to their definitions, we can easily transform the optimization model to an MOP with the objective functions to be minimized. According to the above analysis, we formulate the optimization model as

$$\begin{array}{ll} \text{mimimize} & \mathbf{F}(\mathbf{x}) = [1 - D_{\mu}^{r}(\mathbf{x}), 1 - D_{\sigma}^{r}(\mathbf{x})]^{T} \\ \text{subject to} & \mathbf{x} \in \mathbb{X} \end{array}, \tag{18}$$

where $\mathbf{x}$ denotes the vector of the input (decision) variables, $\mathbb{X}$ denotes the design space of input variables, and $D_{\mu}^{r}(\mathbf{x})$ and $D_{\sigma}^{r}(\mathbf{x})$ are the overall robust desirability functions defined in Eqs. (15) and (17), respectively.

4. Proposed optimization algorithm: NSGAII-DMS

This section proposes a multi-objective optimization algorithm called NSGAII-DMS that combines the search mechanisms of NSGA-II and DMS for solving the proposed MRO model. We first introduce the overall procedure of NSGAII-DMS, and then, introduce the main components of NSGAII-DMS in detail.

4.1. Overall procedure of NSGAII-DMS

NSGA-II is a competitive multi-objective optimization algorithm with good global search performance, while DMS performs well on the local search. To solve the established MRO model in Eq. (18), we propose a hybrid optimization algorithm (i.e., NSGAII-DMS) combing the search mechanisms of NSGA-II and DMS. The proposed optimization algorithm has two optimization phases. In the first phase, NSGA-II is adopted to find a set of non-dominated solutions. In the second phase, the poll step in DMS is used to further tune the non-dominated solutions found by NSGA-II. The first phase of NSGAII-DMS can be seen as an exploration process and the second phase of NSGAII-DMS can be seen as an exploitation process. Thus, NSGAII-DMS has the potential to obtain promising optimization results.

The procedure of NSGAII-DMS is shown in Algorithm 1. The NSGA-II process performs in the first phase of NSGAII-DMS. First, the initial population $\mathbb{P}^{t}$ $(t = 1)$ that contains N feasible solutions $\mathbf{x}_{k}^{t}$, $k = 1, 2, ..., N$ is randomly generated. Then, at each iteration, the offspring population $\mathbb{O}^{t}$ is generated by the genetic operators based on the parent population $\mathbb{P}^{t}$ and the sorting pool $\mathbb{S}$ is generated as the union of $\mathbb{O}^{t}$ and $\mathbb{P}^{t}$. After that, we sort the solutions in $\mathbb{S}$ using the fast non-dominated sorting approach and the crowding distance measure (see Section 4.3), and then, add the best N solution to the population $\mathbb{P}^{t+1}$ of the next generation. Finally, after the iterations, the NSGA-II process finds a set L_{ns} of non-dominated solutions, which is input of the next phase, i.e., the DMS process.

The DMS process performs in the second phase of NSGAII-DMS. First, an initial step size parameter α_0 is assigned to each solution in the non-dominated set L_{ns}. Then, at each iteration, a set L_{trial} of new

solutions is generated based on Eq. (3) described in Section 2.3. Next, the original non-dominated set L_{ns} is updated by the new solutions based on the Pareto dominance concept. It should be noted that we let the maximum size of the non-dominated set L_{ns} be N (equal to the population size). Thus, the problem that the non-dominated set L_{ns} gradually gets extremely large during the iterations can be avoided. Specifically, if the number of solutions in L_{ns} exceeds N, we eliminate the solutions with the largest crowding distance value (shown in Eq. (19)) to make the size of L_{ns} be N. Finally, when the number of the function evaluations of the DMS process reaches the predefined maximum evaluation number E, the whole algorithm terminates.

Algorithm 1: Pseudocode of NSGAII-DMS.

Input : The maximum number of generations during the NSGA-II process T, the population size N, the maximum number of the function evaluations during the DMS process E, and the initial value of the step size parameter α_0 ;

Output : The set of found non-dominated solutions L_{ns};

`/* Begin the NSGA-II process. */`

$t \leftarrow 1$; `/* Initialize the generation counter` t `*/`

$\mathbb{P}^t \leftarrow \{\mathbf{x}_1^t, \mathbf{x}_2^t, ..., \mathbf{x}_N^t\}$; `/* Initialize the population` $\mathbb{P}^t$`. ` $\mathbf{x}_k^t$ `(`$k = 1, ..., N$`) denotes a feasible solution. */`

Evaluate the two objective functions based on Eq. (18) for each $\mathbf{x}_k^t \in \mathbb{P}^t$;

Sort the solutions in $\mathbb{P}^t$ based on the *fast non-dominated sorting* approach and the *crowding distance* measure (see Section 4.3);

while $t < T$ **do**

  Generate the offspring population $\mathbb{O}^t$ by applying genetic operators on $\mathbb{P}^t$ (see Section 4.4);

  Evaluate the two objective functions based on Eq. (18) for each solution in $\mathbb{O}^t$;

  $\mathbb{S} \leftarrow \mathbb{O}^t \cup \mathbb{P}^t$; `/* Generate the sorting poll` $\mathbb{S}$ `*/`

  $\mathbb{P}^{t+1} \leftarrow$ Sort the solutions in $\mathbb{S}$ using the *fast non-dominated sorting* approach and the *crowding distance* measure and return the best N solutions (see Section 4.3);

  $t \leftarrow t + 1$;

end

$L_{ns} \leftarrow$ The non-dominated solutions in $\mathbb{P}^t$;

`/* Begin the DMS process. */`

$e \leftarrow 0$; `/* Initialize the function evaluation counter` e `of the DMS process. */`

For each solution $\mathbf{X} \in L_{ns}$, assign the step size parameter value as $\alpha_{\mathbf{X}} = \alpha_0$;

while $e < E$ **do**

  Select a poll center $\mathbf{x}_p$ from L_{ns} (see Section 4.5);

  Randomly generate a postive spanning set D;

  $L_{trial} \leftarrow \{\mathbf{x}_p + \alpha_{\mathbf{x}_p}\mathbf{d} | \mathbf{d} \in D\}$; `/* Generate a set` L_{trial} `of new solutions based on the poll step. */`

  Evaluate the two objective functions of each solution in L_{trial} based on Eq. (18);

  Update the non-dominated set L_{ns} with L_{trial};

  Update the step size parameter value of the poll center $\mathbf{x}_p$ from $\alpha_{\mathbf{x}_p}$ to $\alpha_{\mathbf{x}_{p,new}}$ (see Section 4.6);

  For each solution $\mathbf{x} \in L_{ns}$, let $\alpha_{\mathbf{x}} = \alpha_{\mathbf{x}_p}$ if $\mathbf{x} = \mathbf{x}_p$ *or* $\mathbf{x} \in L_{trial}$;

  $e \leftarrow e + |D|$; `/* Update the function evaluation counter` e`. ` $|D|$ `denotes the number of vectors in` D`. */`

end

return The set of non-dominated solutions L_{ns};

Algorithm 2: Pseudocode of the fast non-dominated sorting approach.

Input : The sorting poll $\mathbb{S}$;
Output : Non-dominated fronts $\mathbb{F}_1, \mathbb{F}_2, ..., \mathbb{F}_l$;

```
i ← 0 ;
while 𝕊 ≠ ∅ do
    i ← i + 1 ;
    𝔽_i ← Find the non-dominated solutions from 𝕊 ;
    𝕊 ← 𝕊\𝔽_i ;
end
l ← i ;
return Non-dominated fronts 𝔽_1, 𝔽_2, ..., 𝔽_l ;
```

4.2. Solution encoding and initialization

In NSGAII-DMS, the real encoding strategy is used to represent solutions. In the RSM scenario, the design space of the input variables is generally a cuboid region $-1 \leq x_i \leq 1$ $(i = 1, 2, ..., n)$. Therefore, the input variables for the MRO problem can be represented as a vector $\mathbf{x} = [x_1, x_2, ..., x_n]^T$ where each $-1 \leq x_i \leq 1$, $i = 1, 2, ..., n$.

To initialize a feasible solution $\mathbf{x} = [x_1, x_2, ..., x_n]^T$, we set the value of each x_i $(i = 1, 2, ..., n)$ as a random value from the uniform distribution $U(-1, 1)$. It is also worth noting that, during the iterations of NSGAII-DMS, the new generated solutions may be out of the feasible solution space (i.e., $x_i < -1$ or $x_i > 1$). To address this issue, we further use a repairing strategy that replaces the original value of x_i with -1 if $x_i < -1$ and replaces the original value of x_i with 1 if $x_i > 1$.

4.3. Sorting solutions

In NSGAII-DMS, the fast non-dominated sorting approach and the crowding distance measure proposed by Deb et al. (2002) is used to sort solutions with respect to their goodness.

The main procedure of the fast non-dominated sorting approach is shown in Algorithm 2. First, this sorting approach selects the non-dominated solutions from the original sorting poll $\mathbb{S}$ and appends them into the first non-dominated front $\mathbb{F}_1$. Then, the sorting poll $\mathbb{S}$ is updated by removing the solutions in $\mathbb{F}_1$. Next, the second non-dominated front $\mathbb{F}_2$ is constructed in the same way as $\mathbb{F}_1$ and $\mathbb{S}$ is further updated by removing the solutions in $\mathbb{F}_2$. This process continues until $\mathbb{S}$ is empty and we finally divide the original solutions in $\mathbb{S}$ into l fronts $\mathbb{F}_1, \mathbb{F}_2, ..., \mathbb{F}_l$. Given two solutions $\mathbf{x}_1 \in \mathbb{F}_a$ and $\mathbf{x}_2 \in \mathbb{F}_b$, $\mathbf{x}_1$ is better than $\mathbf{x}_2$ if $a < b$.

The crowding distance of a solution is calculated as the average side length of the cuboid composed by its two nearest solutions in the same non-dominated front. Let $\mathbf{x} \in \mathbb{F}_i$ be a solution in the non-dominated front i $(i \in \{1, 2, ..., l\})$, and $\mathbf{x}^+ \in \mathbb{F}_i$ and $\mathbf{x}^- \in \mathbb{F}_i$ be its two nearest solutions in the same front. Then, the

crowding distance value of $\mathbf{x}$ is calculated as

$$cd(\mathbf{x}) = \begin{cases} \infty; & if \quad \exists j \in \{1,2,..,m\} : f_j(\mathbf{x}) = f_j^{\max} \quad or \quad f_j(\mathbf{x}) = f_j^{\min} \\ \sum_{j=1}^{m} \frac{|f_j(\mathbf{x}^+) - f_j(\mathbf{x}^-)|}{f_j^{\max} - f_j^{\min}}; & otherwise \end{cases} \tag{19}$$

where $f_j^{\max} = \max_{\mathbf{q} \in \mathbb{F}_i} f_j(\mathbf{q})$ and $f_j^{\min} = \min_{\mathbf{q} \in \mathbb{F}_i} f_j(\mathbf{q})$. The crowding distance $cd(\mathbf{x})$ indicates the density of solutions in the local area around $\mathbf{x}$. It can be used to compare any two solutions in the same non-dominated front. A larger crowding distance value denotes a better fitness level of the solution.

In NSGAII-DMS, we can sort the solutions in the sorting poll $\mathbb{S}$ according to solutions' goodness evaluated by the aforementioned fast non-dominated sorting approach and the crowding distance measure, and then, add the best N solutions to the population $\mathbb{P}^{t+1}$ as shown in line 9 of Algorithm 1. It should be noted that, in this paper, we use a dynamic crowding distance calculation strategy (Luo et al., 2008) to select the best N solutions from $\mathbb{S}$. In this dynamic strategy, we first obtain the non-dominated fronts with the fast non-dominated sorting approach and obtain the crowding distance with Eq. (19) for each solution. Next, the worst solution (the one that has the smallest crowding distance value in the last non-dominated front) is eliminated. After the elimination, we use Eq. (19) again to update the crowding distance value for each remaining solution. Then, the worst solution determined by the updated crowding distances is eliminated. This process continues until the number of remaining solutions equals N. The remaining solutions are the best N solutions to be added to $\mathbb{P}^{t+1}$. Compared with the static crowding distance calculation strategy, which calculates the crowding distance for each solution once, the dynamic one has the advantage of producing more uniformly distributed solutions.

4.4. Genetic operators

In NSGAII-DMS, we use binary tournament selection, simulated binary crossover (SBX) operator, and the polynomial mutation (PM) operator to conduct genetic operations as that used in Deb et al. (2002). In an iteration of the NSGA-II process, the tournament selection strategy is first used to select parent solutions. Then, the SBX and PM operators are utilized to generate offspring solutions based on the selected parent solutions. A brief introduction of the genetic operators is shown below.

The binary tournament selection strategy conducts N tournament selections to select N parent solutions from the population. During each tournament selection, two solutions are first selected from the population at random, and then, the one with a better fitness level is selected as the parent solution. The selected parent solutions are then randomly mated into $N/2$ pairs, which are further used by the following crossover and mutation operators.

The SBX operator generates two offspring solutions based on a pair of parent solutions with a crossover probability of p_c. Let $\mathbf{x}_1 = [x_{1,1}, x_{1,2}, ..., x_{1,n}]^T$ and $\mathbf{x}_2 = [x_{2,1}, x_{2,2}..., x_{2,n}]^T$ be two paired parent solutions.

The SBX operator is applied to the ith ($i = 1, 2, ..., n$) variable of $\mathbf{x}_1$ and $\mathbf{x}_2$ with a probability of 0.5, which update $x_{1,i}$ and $x_{2,i}$ into

$$\begin{cases} x_{1,i}^{new} = 0.5[(1+\gamma)x_{1,i} + (1-\gamma)x_{2,i}] \\ x_{2,i}^{new} = 0.5[(1-\gamma)x_{1,i} + (1+\gamma)x_{2,i}] \end{cases}. \tag{20}$$

In Eq. (20), γ is a spread factor which is defined as

$$\gamma = \begin{cases} (2u)^{\frac{1}{\eta_c+1}}; & if \quad u \leq 0.5 \\ \left(\frac{1}{2(1-u)}\right)^{\frac{1}{\eta_c+1}}; & otherwise \end{cases} \tag{21}$$

where u is a random number in (0,1) and η_c in the distribution index for the SBX operator.

The PM operator further updates each variable in a solution after the application of the crossover operator. For a solution $\mathbf{x} = [x_1, x_2, ..., x_n]^T$, with a crossover probability of p_m, a variable x_i ($i = 1, 2, ..., n$) is updated into

$$x_i^{new} = x_i + \delta(u_i - l_i), \tag{22}$$

where u_i and l_i are the upper bound and lower bound of the ith variable in the encoded solution of NSGAII-DMS. The δ in Eq. (22) is obtained as

$$\delta = \begin{cases} \left[2u + (1-2u)(1-\delta_1)^{\eta_m+1}\right]^{\frac{1}{\eta_m+1}} - 1; & if \quad u \leq 0.5 \\ 1 - \left[2(1-u) + 2(u-0.5)(1-\delta_2)^{\eta_m+1}\right]^{\frac{1}{\eta_m+1}}; & otherwise \end{cases} \tag{23}$$

where u is a random number in (0,1), η_m in the distribution index for the PM operator, and δ_1 and δ_2 are defined as $\delta_1 = (x_i - l_i)/(u_i - l_i)$ and $\delta_2 = (u_i - x_i)/(u_i - l_i)$.

4.5. Poll center selection strategy

The selection of the poll center at each iteration affects the performance of the DMS process. In this paper, we use the poll center selection strategy suggested by Li et al. (2020). Specifically, each solution in L_{ns} uses a parameter ω to record the number of times that this solution is selected as the poll center. Then, the solution with the smallest ω value is selected as the poll center at an iteration. This setting makes the poll step searches around different areas of the search space in turn, which can avoid the problem of repeatably searching around some areas of the search space. If there is more than one solution with the smallest ω value, we select the solution with the largest crowding distance. It means the poll step prefers to search in the sparse local area of the search space with a few solutions.

Table 1: Details of the CGA dataset.

Run	Replication	x_1	x_2	x_3	y_1	y_2	y_3	Run	Replication	x_1	x_2	x_3	y_1	y_2	y_3
1	1	-1	-1	-1	4.50	0.17	29.00	10	1	1	0	0	5.52	0.52	30.00
	2	-1	-1	-1	4.50	0.26	23.00		2	1	0	0	5.39	0.51	24.00
2	1	1	-1	-1	6.04	0.50	23.00	11	1	0	-1	0	5.92	0.61	32.00
	2	1	-1	-1	6.39	0.53	25.40		2	0	-1	0	5.93	0.59	23.40
3	1	-1	1	-1	3.81	0.17	22.00	12	1	0	1	0	4.74	0.36	36.00
	2	-1	1	-1	4.09	0.20	27.00		2	0	1	0	4.50	0.30	21.00
4	1	1	1	-1	5.67	0.44	25.50	13	1	0	0	-1	5.01	0.36	27.00
	2	1	1	-1	5.19	0.40	21.00		2	0	0	-1	4.70	0.25	24.00
5	1	-1	-1	1	4.67	0.32	20.00	14	1	0	0	1	4.94	0.53	38.00
	2	-1	-1	1	4.22	0.32	41.00		2	0	0	1	5.01	0.51	25.00
6	1	1	-1	1	6.73	0.57	35.50	15	1	0	0	0	4.85	0.47	34.00
	2	1	-1	1	6.57	0.57	18.00		2	0	0	0	4.94	0.46	34.00
7	1	-1	1	1	3.40	0.12	43.00		3	0	0	0	4.98	0.49	33.00
	2	-1	1	1	4.32	0.28	20.00		4	0	0	0	4.89	0.48	24.00
8	1	1	1	1	5.72	0.46	19.00		5	0	0	0	4.94	0.46	19.00
	2	1	1	1	5.09	0.50	34.00		6	0	0	0	5.01	0.47	25.00
9	1	-1	0	0	4.09	0.27	36.00								
	2	-1	0	0	4.38	0.23	24.00								

4.6. Step size parameter update strategy

As we stated in Section 2.3, the step size parameter $\alpha_{\mathbf{x}_p}$ of the poll center should be updated after each iteration. As suggested by Custódio et al. (2011), we set $\alpha_{\mathbf{x}_{p,new}} = \mathbf{x}_p$ if the generated L_{trial} successfully updates the current non-dominated set L_{ns} and set $\alpha_{\mathbf{x}_{p,new}} = \beta \mathbf{x}_p$ if L_{trial} fails to update L_{ns}, where $\beta < 1$ is a user-defined parameter. This means the step size is maintained at successful iterations and is reduced at failure iterations.

5. Evaluating the performance of the proposed MRO model

This section verifies the proposed model with two test examples. In the following subsections, the introduction of the test examples, parameter setting, benchmark methods, optimization results of the two examples, the strategy to select the best compromise solution, and the discussion are given.

5.1. Test examples

5.1.1. Example 1: a production process of colloidal gas aphrons (CGAs)

A real MRO problem from a production process of colloidal gas aphrons (CGAs) is used as the first test example. This problem was first reported by Jauregi et al. (1997) and then used by Kim & Lin (2006), He et al. (2017), and Lee et al. (2018) to evaluate the performance of MRO methods. The CGAs are microbubbles composed of a gaseous inner core covered by a thin surfactant film produced by intensively stirring a surfactant solution (Jauregi et al., 1997). The quality of a CGA is measured by three response variables, i.e., stability y_1, volumetric ratio y_2, and temperature y_3. These three responses are the LTB, STB, and NTB types, respectively. The input variables in the experiment are concentration of surfactant x_1, concentration of salt x_2, and time of stirring x_3. The purpose of this example is to find an optimal setting for the three input variables by optimizing both the location and dispersion effects of the responses.

In the experiment, a central composite design (CCD) with 8 factorial points, 6 axial points, and 1 center point is adopted. The center point was replicated 6 times and the other points were replicated twice. Thus, both the mean and standard deviation for each point are obtained and the response models for both the location and dispersion effects can be fitted. The details of the CGA dataset is shown in Table 1, where the coded values for the input variables are shown and the measurement units for the three responses are $y_1 = \log(\text{seconds})$, $y_2 = \text{none (ratio)}$, and $y_3 = {}^\circ\text{C}$.

The means and standard deviations of responses y_1, y_2, and y_3 at each point are estimated based on the samples from the experiment shown in Table 1. We use the ordinary least squares (OLS) method to obtain the regression models. The fitted models are

$$\hat{y}_{1,\mu}(\mathbf{x}) = 4.953 + 0.817x_1 - 0.447x_2 - 0.156x_1^2 + 0.271x_2^2 - 0.112x_1x_2 + 0.069x_1x_3, \tag{24}$$

$$\hat{y}_{2,\mu}(\mathbf{x}) = 0.459 + 0.133x_1 - 0.061x_2 + 0.045x_3 - 0.065x_1^2 - 0.035x_3^2, \tag{25}$$

$$\hat{y}_{3,\mu}(\mathbf{x}) = 28.746 - 1.480x_1 + 2.330x_3 - 0.781x_1^2 - 1.181x_2^2 - 0.712x_1x_3, \tag{26}$$

$$\hat{y}_{1,\sigma}(\mathbf{x}) = 0.059 + 0.112x_2 + 0.057x_3 + 0.118x_1^2 + 0.104x_3^2 - 0.100x_1x_3 + 0.047x_2x_3, \tag{27}$$

$$\hat{y}_{2,\sigma}(\mathbf{x}) = 0.021 - 0.014x_1 + 0.013x_2 - 0.006x_3 + 0.016x_3^2 - 0.006x_1x_3 + 0.022x_2x_3, \tag{28}$$

$$\hat{y}_{3,\sigma}(\mathbf{x}) = 6.082 - 1.527x_1 + 0.495x_2 + 4.851x_3 + 2.262x_2^2 - 0.654x_1x_3 - 0.672x_1x_2x_3, \tag{29}$$

where $\hat{y}_{j,\mu}(\mathbf{x})$ denotes the fitted location effect model for the mean of response y_j, and $\hat{y}_{j,\sigma}(\mathbf{x})$ denotes the fitted dispersion effect model for the standard deviation of response y_j, $j = 1, 2, 3$.

The specifications, including the targets ($T_{j,\mu}$ and $T_{j,\sigma}$), upper limits ($y_{j,\mu}^{\max}$ and $y_{j,\sigma}^{\max}$) and lower limits ($y_{j,\mu}^{\min}$ and $y_{j,\sigma}^{\min}$) for the means and standard deviations of the responses y_i ($j = 1, 2, 3$) are shown in Table 2. The values in Table 2 are set based on the work by Kim & Lin (2006). The only difference is that we relaxed the upper limits of the standard deviations of the responses, i.e., $y_{1,\sigma}^{\max}$, $y_{2,\sigma}^{\max}$, and $y_{3,\sigma}^{\max}$ are changed from 0.10, 0.10, and 2.00 to 0.20, 0.20, and 3.00. The reason for this change is that the worst-case standard deviations considering model uncertainty in the proposed method are larger than that without considering model uncertainty. During the optimization process, the standard deviations of solutions considering model uncertainty generally exceed the original upper limits, which makes the desirability function loses efficacy if the original tight limits are used. Note that, since the standard deviation of each response is the STB type, and the target and lower limit for each standard deviation are the same as that used by Kim & Lin (2006), the optimization objective for the standard deviations of the responses does not change.

5.1.2. Example 2: a synthetic MRO problem

Besides the CGA example, we propose a synthetic MRO problem to further verify the proposed method. The details of the designed experiment and the response values for each input parameter setting for this

Table 2: Specification information of the responses in the CGA Example.

Response	$T_{j,\mu}$	$y_{j,\mu}^{\min}$	$y_{j,\mu}^{\max}$	$T_{i,\sigma}$	$y_{j,\sigma}^{\min}$	$y_{j,\sigma}^{\max}$
y_1 (LTB)	7.00	3.00	7.00	0.00	0.00	0.20
y_2 (STB)	0.10	0.10	0.60	0.00	0.00	0.20
y_3 (NTB)	30.00	15.00	45.00	1.00	1.00	3.00

Table 3: Details of the synthetic dataset.

Run	Replication	x_1	x_2	x_3	y_1	y_2	y_3	Run	Replication	x_1	x_2	x_3	y_1	y_2	y_3
1	1	-1	-1	-1	30.74	51.26	9.92	10	1	1	0	0	32.10	51.64	10.70
	2	-1	-1	-1	28.65	50.11	9.61		2	1	0	0	30.38	50.76	10.29
2	1	1	-1	-1	34.47	41.00	11.21	11	1	0	-1	0	34.83	52.54	11.25
	2	1	-1	-1	32.58	39.87	11.18		2	0	-1	0	33.16	51.29	11.02
3	1	-1	1	-1	26.58	48.08	9.08	12	1	0	1	0	32.41	47.52	9.46
	2	-1	1	-1	24.72	46.63	8.74		2	0	1	0	30.62	46.21	9.05
4	1	1	1	-1	28.72	47.56	9.01	13	1	0	0	-1	29.60	48.45	9.59
	2	1	1	-1	26.96	46.56	8.84		2	0	0	-1	27.50	47.25	9.32
5	1	-1	-1	1	31.22	54.14	11.09	14	1	0	0	1	28.21	51.31	10.50
	2	-1	-1	1	29.60	53.41	11.03		2	0	0	1	26.56	50.29	10.24
6	1	1	-1	1	33.99	48.07	10.83	15	1	0	0	0	29.49	53.19	8.98
	2	1	-1	1	32.58	47.09	10.35		2	0	0	0	29.67	52.15	9.22
7	1	-1	1	1	27.41	52.52	12.01		3	0	0	0	30.57	52.01	9.10
	2	-1	1	1	25.68	51.49	11.79		4	0	0	0	29.34	51.38	9.38
8	1	1	1	1	28.64	51.40	12.30		5	0	0	0	31.59	53.12	9.20
	2	1	1	1	26.82	50.00	11.78		6	0	0	0	27.51	52.12	8.67
9	1	-1	0	0	29.16	50.98	10.16								
	2	-1	0	0	27.28	50.03	9.95								

synthetic MRO problem are shown in Table 3. The specification information of the three responses in the synthetic example is shown in Table 4. The three responses y_1, y_2, and y_3 are LTB, NTB, and STB types, respectively. This synthetic MRO problem aims to find a good parameter setting for the three input variables x_1, x_2, and x_3 while simultaneously optimizing these responses with respect to the specification information. Moreover, as shown in Table 3, a central composite design (CCD) with 8 factorial points, 6 axial points, and 1 center point is adopted. The center point is replicated 6 times and the other points are replicated twice. Thus, we can compute the mean and standard deviation for each point to obtain the location effect and dispersion effect regression models, which are used in the optimization process of the MRO methods. The fitted regression models with the OLS method are shown as

$$\hat{y}_{1,\mu}(\mathbf{x}) = 30.469 + 1.288x_1 - 1.858x_2 + 2.160x_2^2 - 2.883x_3^2 - 1.403x_1x_3, \tag{30}$$

$$\hat{y}_{2,\mu}(\mathbf{x}) = 48.593 - 2.176x_1 + 2.407x_3 + 2.204x_3^2 - 2.671x_1x_3, \tag{31}$$

$$\hat{y}_{3,\mu}(\mathbf{x}) = 10.179 - 0.493x_2 + 0.760x_3 - 0.988x_1^2 + 0.724x_2^2 + 0.932x_2x_3, \tag{32}$$

$$\hat{y}_{1,\sigma}(\mathbf{x}) = 1.331 + 0.143x_2 - 0.090x_3 - 0.210x_2^2 + 0.183x_3^2 + 0.088x_2x_3, \tag{33}$$

$$\hat{y}_{2,\sigma}(\mathbf{x}) = 0.832 - 0.037x_1 + 0.058x_2 - 0.042x_3 - 0.066x_1^2 + 0.107x_1x_3, \tag{34}$$

$$\hat{y}_{3,\sigma}(\mathbf{x}) = 0.201 + 0.066x_1 + 0.076x_3 - 0.119x_1x_2 + 0.079x_1x_3, \tag{35}$$

where $\hat{y}_{j,\mu}(\mathbf{x})$ and and $\hat{y}_{j,\sigma}(\mathbf{x})$ are the fitted location effect and dispersion effect models for response y_j, $j = 1, 2, 3$.

Table 4: Specification information of the responses in the synthetic example.

Response	$T_{j,\mu}$	$y_{j,\mu}^{\min}$	$y_{j,\mu}^{\max}$	$T_{i,\sigma}$	$y_{j,\sigma}^{\min}$	$y_{j,\sigma}^{\max}$
y_1 (LTB)	35.00	25.00	35.00	0.50	0.50	1.50
y_2 (NTB)	50.00	40.00	60.00	0.00	0.00	0.70
y_3 (STB)	5.00	5.00	15.00	0.00	0.00	0.20

5.2. Parameter setting

NSGAII-DMS is composed of the NSGA-II and the DMS processes. Since the DMS process can be seen as a separate process further tuning the solutions returned by the NSGA-II process, it does affect the inner search mechanism of the NSGA-II process. Therefore, the parameters used in the NSGA-II process of NSGAII-DMS are set based on the NSGA-II algorithm that is used in Deb et al. (2002). These parameters in NSGA-II are well-tuned and widely used in many optimization problems. Specifically, the population size is set as $N = 100$, the crossover probability is set as $p_c = 0.9$, the mutation probability is set as $p_c = 1/n$ (n is the number of input variables), and the distribution indices for the cross and mutation operators are set as $\eta_c = 20$ and $\eta_m = 20$.

The total number of function evaluations of NSGAII-DMS is set as 25,000, which is the same as Deb et al. (2002). However, since NSGAII-DMS is composed of the NSGA-II and DMS processes. We need to further tune the number of generations T of the NSGA-II process and the number of function evaluations E of the DMS process. Moreover, the parameters used in the DMS process are the initial step size parameter α_0, and the parameter β that controls the change of the step size. The original study of DMS by Custódio et al. (2011) sets $\alpha_0 = 1$ and $\beta = 0.5$, which means a relatively large initial step size is used to ensure the global search performance of DMS and the step size is halved at failure iterations. We have conducted several initial experiments which have shown that these parameters are not suitable for NSGAII-DMS. This is because, in NSGAII-DMS, we have already used the NSGA-II process to globally update solutions before the DMS process. Thus, it would be better to use a relatively small α_0 value to make the DMS process focus on the local search. Therefore, the two parameters α_0 and β should be further tuned.

According to the above analysis, four parameters are required to be further tuned. They are the number of generations T of the NSGA-II process, the number of function evaluations E of the DMS process, and the parameters α_0 and β in the DMS process. Moreover, since T and E should meet the constraint $100 * T + E = 25,000$ (25,000 is the total number of function evaluations), we only need to tune three parameters for NSGAII-DMS, i.e., T, α_0, and β. The details of the experiments that tune the three parameters are shown in Appendix Appendix A. Based on the tuning experiments, we obtain the following desirable parameter values: $T = 100$, $\alpha_0 = 0.4$, and $\beta = 0.85$. Then, with the constraints $100 * T + E = 25,000$ we obtain $E = 15,000$. Finally, we obtain a desirable parameter setting for NSGAII-DMS, i.e., population size $N = 100$, maximum number of generations of the GA process $T = 100$, crossover probability $P_c = 0.9$, mutation probability $P_m = 1/n$, maximum number of function evaluations of the DMS process $E = 15,000$,

initial step size parameter $\alpha_0 = 0.4$, and the parameter for updating the step size $\beta = 0.85$. This parameter setting will be used in the following experiments.

5.3. Benchmark methods

Six MRO methods, denoted by TDF (Derringer, 1994), FDF1 (Kim & Lin, 2000), FDF2 (Kim & Lin, 2006), RDF (He et al., 2012), RFDF (He et al., 2017), and MDF (Lee et al., 2018), are adopted as the benchmark methods to verify the performance of the proposed model. TDF is the traditional desirability function method that optimizes the location effect of multiple responses. FDF1 is a fuzzy desirability function method that optimizes the location effect of multiple responses. FDF2 is a variant of FDF1 that considers both the location and dispersion effects of MRO problems. RDF is a robust MRO method that considers the location effect of multiple responses as well as model uncertainty. RFDF is a robust fuzzy desirability function method that considers the location effect, dispersion effect, and model uncertainty for MRO problems. The above four benchmark methods construct an MRO problem as a single objective optimization model and adopt single objective optimization algorithms to find the final solution. In comparison, the MDF method is a multi-objective approach that forms an MRO problem into a multi-objective optimization model. Specifically, the location and dispersion effects of multiple responses are modeled respectively using the desirability functions, and the two effects are simultaneously optimized. It should be noted that the difference between this model and the optimization model in our method is that model uncertainty is additionally considered in our model. To make a fair comparison between the two multi-objective MRO models, the optimization model of MDF is optimized by the same NSGAII-DMS as that is used in our method.

In the two test examples, the methods (including RDF, RFDF, and the proposed method) considering model uncertainty use a moderate family error of 0.4 (in which case the significance level α for each response is around 0.1566) to calculate the confidence intervals to obtain the robust desirability values for the optimization models as suggested by He et al. (2012). Moreover, for all the compared methods, a linear desirability function and the same weight value (i.e., $w_{j,\mu} = w_{j,\sigma} = 1$, $j = 1, 2, 3$) for the three responses are employed to construct desirability functions for the optimization models as suggested by Kim & Lin (2006).

The optimization results of the two examples obtained by the MRO methods will be compared in detail below in Sections 5.4 and 5.5. In the two sections, we first compare the overall robust desirability values on the location and desirability effects of the methods. Then, we compare the solutions' mean and standard deviation values on the responses. Finally, we compare the solutions' worst mean and standard deviation values in the $1-\alpha$ confidence intervals on the responses, which means model uncertainty is considered during the comparison.

5.4. The optimization results of Example 1 (the CGA example)

5.4.1. Comparison of the obtained robust desirability values

Fig. 2 shows the overall robust desirability values of the location (D_μ^r) and dispersion effects (D_σ^r) of the compared methods in . The x-axis denotes the overall robust desirability value of the location effect (based on Eq. (15)) and the y-axis denotes the overall robust desirability value of the dispersion effect (based on Eq. (17)). Each point in the figure denotes the robust desirability value of the location effect and that of the dispersion effect for a solution.

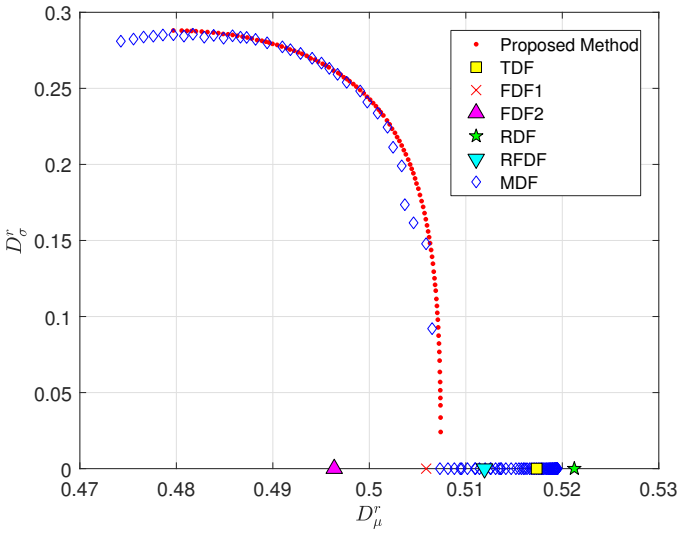

Figure 2: Overall robust desirability values of the location (D_μ^r) and dispersion (D_σ^r) effects obtained by the MRO methods in the CGA example.

According to Fig. 2, the proposed method shows better performance than the benchmark methods. First, the proposed method and the MDF method return a set of solutions instead of one single solution since the two methods are multi-objective MRO methods. Specifically, the proposed method can find solutions with different D_μ^r and D_σ^r values that are well distributed on the non-dominated front. This is because the proposed method simultaneously optimizes D_μ^r and D_σ^r with respect to the location and dispersion effects. The solutions of MDF on the northwest side of the figure are close to the solutions found by the proposed method. However, the solutions of MDF on the southeast side of the figure seem to be undesirable from the perspective of optimizing both the two effects, since the D_σ^r values of these solutions are 0. This denotes that the worst standard deviation values of the solutions of MDF in the $1-\alpha$ confidence intervals predicted by the models do not meet the required specifications because MDF does not consider model uncertainty. Second, the TDF, FDF1, FDF2, RDF, and RFDF methods obtain D_σ^r values of 0. This shows that these methods do not obtain desirable solutions that can meet the standard deviation specifications. One reason that leads to this result is that the TDF, FDF1, and RDF methods do not consider the dispersion effect when

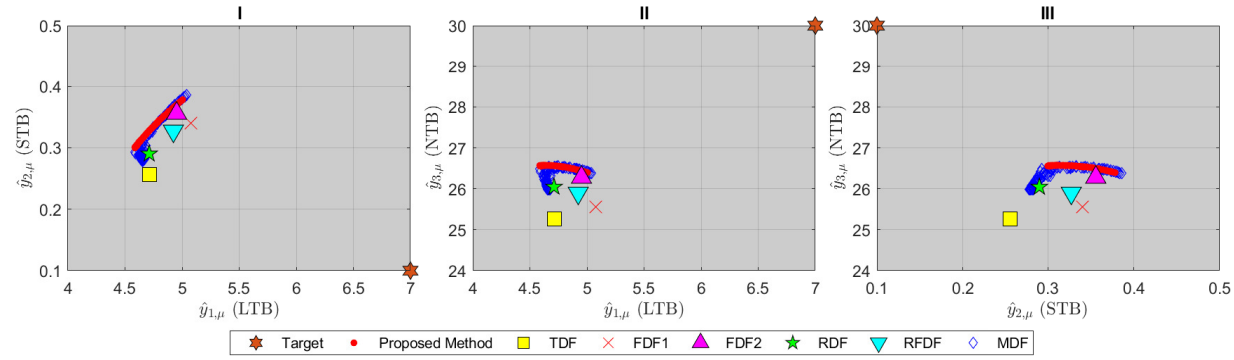

(a) Mean.

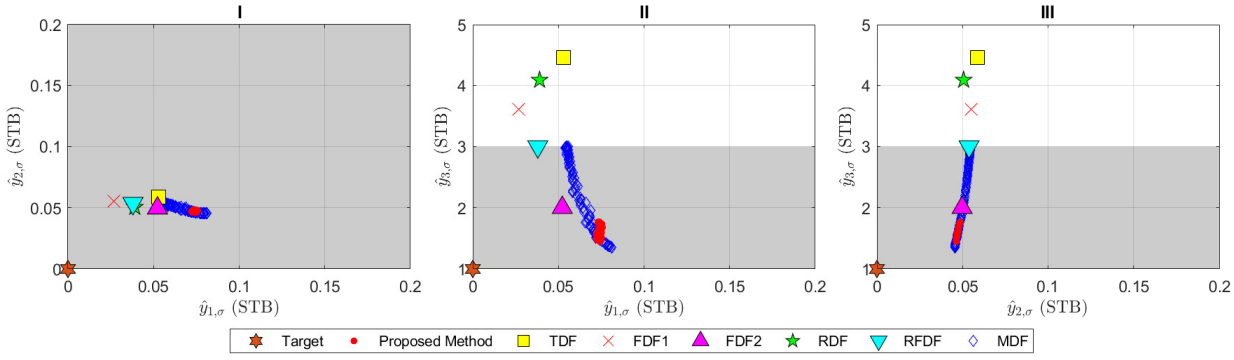

(b) Standard deviation.

Figure 3: Comparison of the mean ($\hat{y}_{j,\mu}$, $j = 1, 2, 3$) and standard deviation ($\hat{y}_{j,\sigma}$, $j = 1, 2, 3$) values of the three responses for the solutions obtained by the MRO methods in the CGA example. The x-axis/y-axis in subfigures (a)-I, (a)-II, and (b)-III are $\hat{y}_{1,\mu}/\hat{y}_{2,\mu}$, $\hat{y}_{1,\mu}/\hat{y}_{3,\mu}$, and $\hat{y}_{2,\mu}/\hat{y}_{3,\mu}$. The x-axis/y-axis in subfigures (b)-I, (b)-II, and (b)-III are $\hat{y}_{1,\sigma}/\hat{y}_{2,\sigma}$, $\hat{y}_{1,\sigma}/\hat{y}_{3,\sigma}$, and $\hat{y}_{2,\mu}/\hat{y}_{3,\sigma}$. The areas that meet the required specifications are marked in gray.

constructing the optimization models. For the FDF2 and RFDF methods, although the dispersion effect is considered when forming the optimization model, the uncertainty of the fitted dispersion effect regression models is not considered, which leads to the bad performance of the obtained solutions. Considering only the location effect, the RDF method obtains the best D_μ^r value because this method establishes an optimization model considering model uncertainty to optimize the mean values (location effect) of the responses.

5.4.2. Comparison of the obtained mean and standard deviation values

In order to give a direct view of the mean and standard deviation results of the solutions obtained by the methods, we show the mean ($\hat{y}_{j,\mu}$, $j = 1, 2, 3$) and standard deviation ($\hat{y}_{j,\sigma}$, $j = 1, 2, 3$) values of the 3 responses for the obtained solutions in Fig 3 (note that the effect of model uncertainty is not shown in the two figures). Specifically, in Figs 3a and 3b, we use three subfigures to show the results. Each subfigure shows the performance of the solutions in terms of two of the three responses.

Several results can be found in Fig. 3a. First, the solutions obtained by the proposed method are close to the solutions obtained by the MDF method. In the meantime, the ranges of the solutions obtained by

the MDF method on the three subfigures are larger than those of the proposed method, which means that the $\hat{y}_{i,\mu}$ values of the solutions of MDF vary more widely than those of the proposed method. This may be because the proposed method adopts stricter constraints in the optimization model by considering model uncertainty, which results in more concentrated solutions shown in Fig. 3a. Second, for the single objective optimization based methods (the methods except for MDF and the proposed method), all the obtained solutions meet the specifications of the responses. It should be noted that these methods have different preferences for the three responses. For example, the TDF method obtains the best (lowest) $\hat{y}_{2,\mu}$ value while obtaining the worst (lowest) $\hat{y}_{3,\mu}$ value. The FDF1 method obtains the highest (best) $\hat{y}_{1,\mu}$ value while obtaining a worse (higher) $\hat{y}_{2,\mu}$ value than the TDF, RDF, and RFDF methods.

According to Fig. 3b, the $\hat{y}_{3,\sigma}$ values of TDF, FDF1, and RDF on response y_3 (i.e., $\hat{y}_{3,\sigma}$) exceed the upper specification limit $y_{3,\sigma}^{\max} = 3.00$. This is because the three methods do not consider the dispersion effect when constructing the optimization models. In comparison, all the $\hat{y}_{j,\sigma}$ $(j = 1, 2, 3)$ values of FDF2, RFDF, MDF, and the proposed method on the responses meet the specifications because these methods consider both the location and dispersion effects. Comparing between the two multi-objective MRO methods, the ranges of the standard deviation values of the solutions obtained by the proposed method are narrower than that of the MDF method. This is because the proposed method adopts the robust overall desirability function that considers model uncertainty to model the location effect instead of the traditional desirability function used by MDF. For the RFDF method, the standard deviation value $\hat{y}_{3,\sigma}$ equals the upper specification limit $y_{3,\sigma}^{\max} = 3.00$. This is because meeting the standard deviation specifications of the responses is used as the constraints in RFDF instead of being used as a part of the objective function in the optimization model.

5.4.3. Comparison of the obtained worst-case mean and standard deviation values considering model uncertainty

The uncertainty caused by the regression models is not shown in Fig 3. To give a more comprehensive view of the performance of the MRO methods, one additional figure, Fig 4, is plotted. In the figure, the robust mean ($\hat{y}_{j,\mu}^{r}$, $j = 1, 2, 3$) and standard deviation ($\hat{y}_{j,\sigma}^{r}$, $j = 1, 2, 3$) results of the methods are shown, which considers the uncertainty of the fitted regression models. Specifically, the $\hat{y}_{j,\mu}^{r}$ value for a solution $\mathbf{x}$ is defined as the worst value (according to the LTB, STB, or NTB type of the response) in the $1 - \alpha$ confidence interval $[y_{j,\mu}^{L}(\mathbf{x}), y_{j,\mu}^{U}(\mathbf{x})]$ (defined in Eq. (9)). The $\hat{y}_{j,\sigma}^{r}$ value for a solution $\mathbf{x}$ is defined as the worst value in the $1 - \alpha$ confidence interval $[y_{j,\sigma}^{L}(\mathbf{x}), y_{j,\sigma}^{U}(\mathbf{x})]$.

According to Fig. 4a, all the robust mean values of the solutions obtained by the compared methods meet the specifications. The relative position of the solutions obtained by the methods shown in Fig. 4a is similar to that shown in Fig. 3a. The difference is that the distances between these solutions and the target are larger than that in Fig. 3a because the robust mean values (i.e., the worst mean value in the confidence interval) are used to show the methods' performance. A similar result is found in Fig. 4b, i.e.,

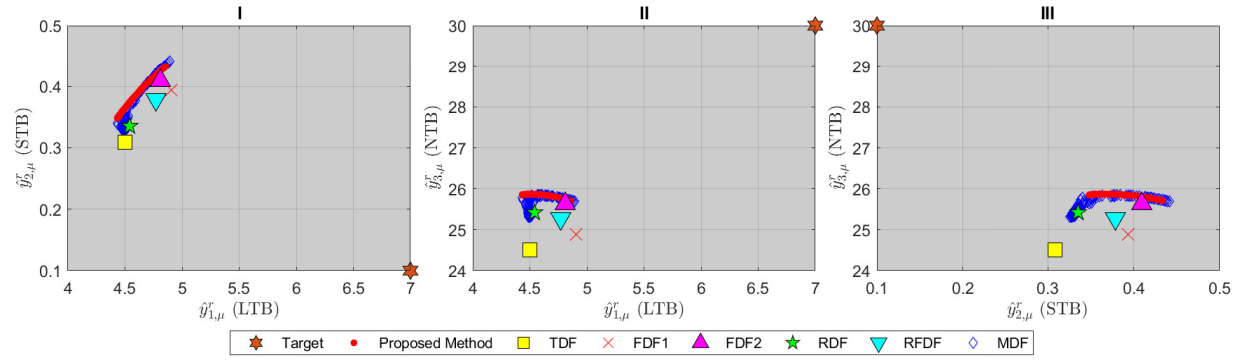

(a) Mean.

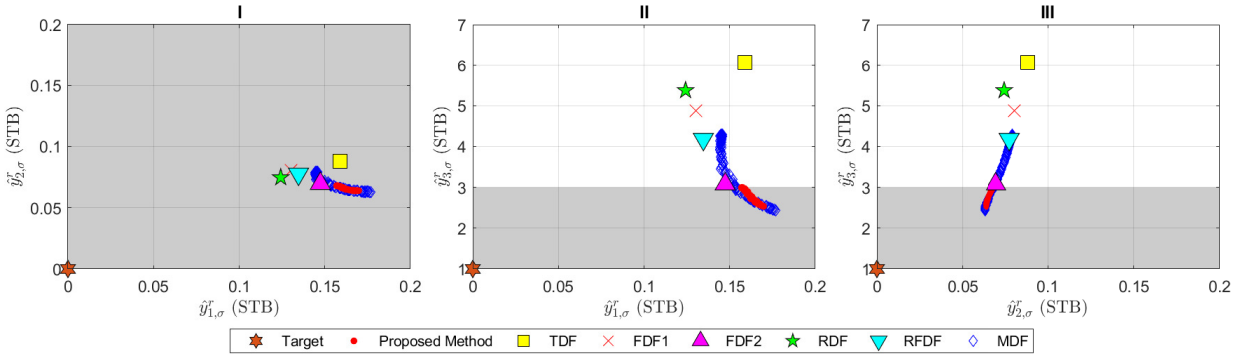

(b) Standard deviation.

Figure 4: Comparison of the robust mean ($\hat{y}^r_{j,\mu}$, $j = 1, 2, 3$) and standard deviation ($\hat{y}^r_{j,\sigma}$, $j = 1, 2, 3$) values of the three responses for the solutions obtained by the MRO methods in the CGA example. The x-axis/y-axis in subfigures (a)-I, (a)-II, and (b)-III are $\hat{y}^r_{1,\mu}/\hat{y}^r_{2,\mu}$, $\hat{y}^r_{1,\mu}/\hat{y}^r_{3,\mu}$, and $\hat{y}^r_{2,\mu}/\hat{y}^r_{3,\mu}$. The x-axis/y-axis in subfigures (b)-I, (b)-II, and (b)-III are $\hat{y}^r_{1,\sigma}/\hat{y}^r_{2,\sigma}$, $\hat{y}^r_{1,\sigma}/\hat{y}^r_{3,\sigma}$, and $\hat{y}^r_{2,\mu}/\hat{y}^r_{3,\sigma}$. The areas that meet the required specifications are marked in gray.

the distances between the solutions and the target in Fig. 4b are larger than that shown in Fig. 3b. The standard deviations of responses y_1 and y_2 (i.e., $\hat{y}^r_{1,\sigma}$ and $\hat{y}^r_{2,\sigma}$) of all the solutions found by the methods meet the specifications. However, on response y_3, only the standard deviations from the solutions of the proposed method are within the upper specification limit (i.e., $y^{\max}_{3,\sigma} = 3.00$). Compared with the results shown in Fig. 3b, the solutions of RFDF and FDF2 as well as partial solutions of MDF also exceed the upper specification limit (i.e., $y^{\max}_{3,\sigma} = 3.00$) in addition to TDF, FDF1, and RDF. This is because even RFDF and MDF consider the location effect of responses, they do not consider model uncertainty. In comparison, the solutions of the proposed method meet all the specifications, which shows that the proposed MRO model performs most effectively by considering model uncertainty.

5.5. The optimization results of Example 2 (the synthetic example)

5.5.1. Comparison of the obtained robust desirability values

Fig. 5 shows the overall robust desirability values of the location (D^r_μ) and dispersion (D^r_σ) effects of the solutions obtained by the compared methods. Each point in the figure denotes the robust desirability

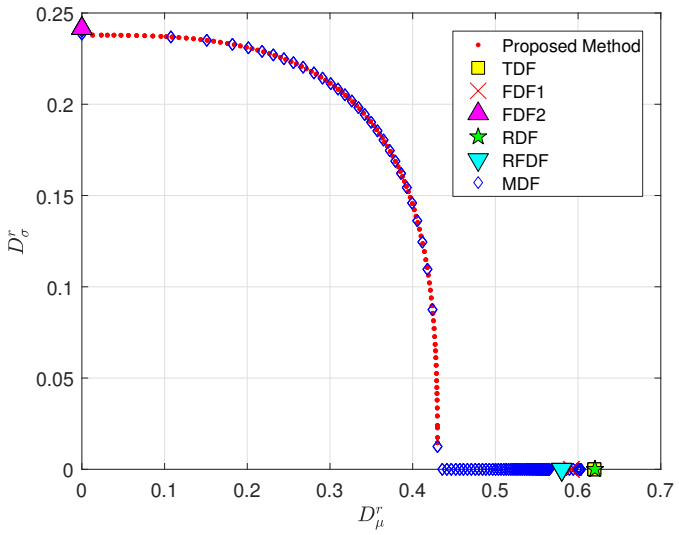

Figure 5: Overall robust desirability values of the location (D^r_μ) and dispersion (D^r_σ) effects obtained by the MRO methods in the synthetic example.

values of the location and dispersion effects for a solution. According to the figure, the proposed method obtains a set of solutions that are well distributed on the non-dominated front. These solutions have different combinations of the D^r_μ and D^r_σ values. In comparison, the benchmark methods do not show desirable D^r_μ and D^r_σ results. First, the TDF, FDF1, RDF, and RFDF methods generally obtain better results on the location effect than the proposed method because the D^r_μ values of these benchmark methods are greater than that of the proposed method. However, the D^r_σ values of these benchmark methods are 0, which means that these methods do not obtain a solution with desirable performance on the dispersion effect. Second, the FDF2 method obtains a better D^r_σ value than the proposed method while obtaining a D^r_μ value of 0. This denotes that the obtained solution of FDF2 does not perform well on the location effect. Finally, similar to the proposed method, the MDF method obtains a set of solutions. Although some solutions of MDF have D^r_μ and D^r_σ values similar to the proposed method, the solutions of MDF on the southeast side of the figure obtain a D^r_σ value of 0. This shows that MDF obtains inferior solutions since it does not consider model uncertainty in the optimization model.

To conclude, the results in Fig. 5 reveal that the proposed method obtains better optimization results on both D^r_μ and D^r_σ in the synthetic example. This shows that our MRO model proposed in Eq.(18) can effectively address the location and dispersion effects while considering model uncertainty.

5.5.2. Comparison of the obtained mean and standard deviation values

Fig. 6 shows the mean ($\hat{y}_{j,\mu}$, $j = 1, 2, 3$) and standard deviation ($\hat{y}_{j,\sigma}$, $j = 1, 2, 3$) values of the responses for the obtained solutions without considering model uncertainty. Similar to that in Section 5.4.2, each subfigure in Fig. 3a or 3b shows the mean or standard deviation results of the obtained solutions in terms

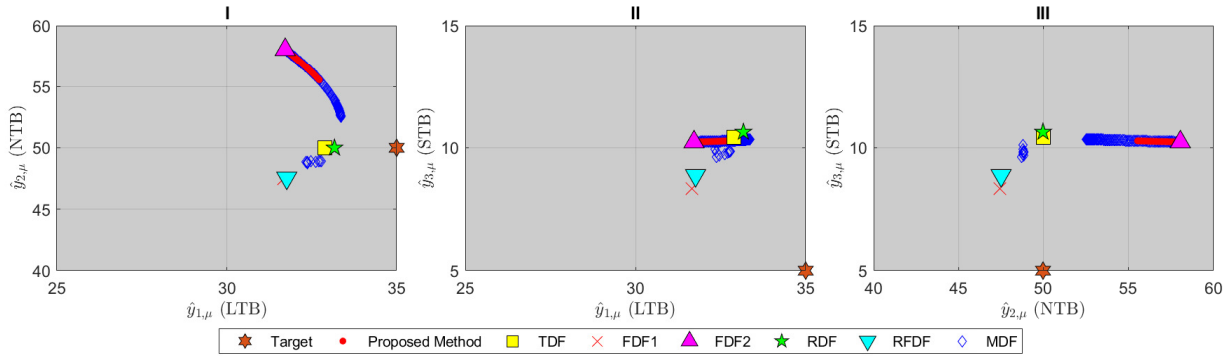

(a) Mean.

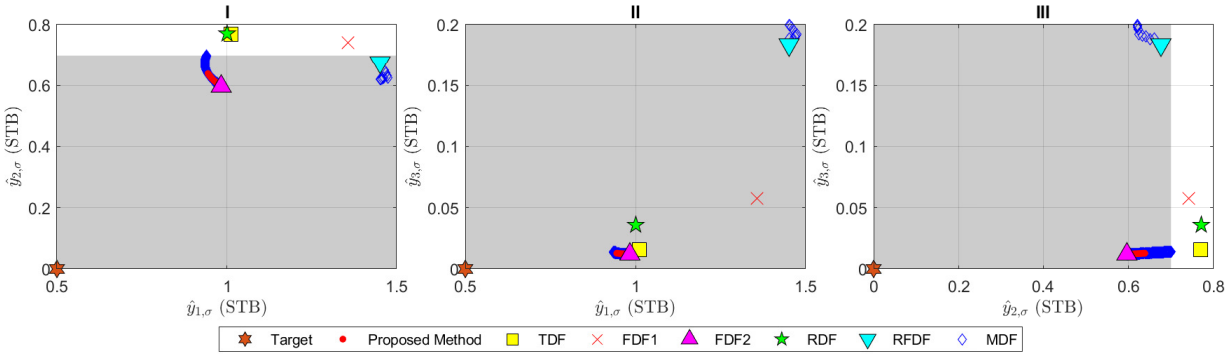

(b) Standard deviation.

Figure 6: Comparison of the mean ($\hat{y}_{j,\mu}$, $j = 1, 2, 3$) and standard deviation ($\hat{y}_{j,\sigma}$, $j = 1, 2, 3$) values of the 3 responses for the solutions obtained by the MRO methods in the synthetic example. The x-axis/y-axis in subfigures (a)-I, (a)-II, and (b)-III are $\hat{y}_{1,\mu}/\hat{y}_{2,\mu}$, $\hat{y}_{1,\mu}/\hat{y}_{3,\mu}$, and $\hat{y}_{2,\mu}/\hat{y}_{3,\mu}$. The x-axis/y-axis in subfigures (b)-I, (b)-II, and (b)-III are $\hat{y}_{1,\sigma}/\hat{y}_{2,\sigma}$, $\hat{y}_{1,\sigma}/\hat{y}_{3,\sigma}$, and $\hat{y}_{2,\mu}/\hat{y}_{3,\sigma}$. The areas that meet the required specifications are marked in gray.

of two of the three responses.

According to Fig. 6a, it is obvious that all the solutions found by the compared methods meet the required specifications since all these methods consider the location effect. Similar to the results in the CGA example, different MRO methods have different preferences. The TDF and RDF methods obtain desirable $\hat{y}_{1,\mu}$ and $\hat{y}_{2,\mu}$ results while obtaining bad $\hat{y}_{3,\mu}$ results. The FDF1 and RFDF methods obtain better $\hat{y}_{3,\mu}$ results while obtaining worse or similar $\hat{y}_{1,\mu}$ results compared with other methods. Moreover, the obtained solutions of MDF and the proposed method are close. However, the ranges of $\hat{y}_{j,\mu}$ ($j = 1, 2, 3$) of MDF are larger than that of the proposed method. This is because the proposed method considers the model uncertainty of the location and dispersion effect models, which narrows its solution space. Finally, the solution of FDF2 is farthest from the target among the solutions obtained by all the methods, which indicates FDF2 obtain the worst results on the location effect. This is because, in this synthetic example, the dispersion effect takes priority over the location effect in FDF2 as we can find in Fig. 5 that FDF2 obtains an excellent D_σ^r value.

According to Fig. 6b, the $\hat{y}_{1,\sigma}$, $\hat{y}_{2,\sigma}$, and $\hat{y}_{3,\sigma}$ values of the proposed method, FDF2, RFDF, and MDF meet the required specifications, whereas the $\hat{y}_{2,\sigma}$ values obtained by TDF, FDF1, and RDF exceed the upper specification limit $y_{2,\sigma}^{\max} = 0.70$. This is because the optimization models of TDF, FDF1, and RDF only consider the location effect while neglecting the dispersion effect. Similar to the results found in the CGA example, the ranges of the standard deviation values obtained by the proposed method are narrower than that of MDF. Specifically, the $\hat{y}_{2,\sigma}$ value of the proposed method is much lower than that of MDF because the proposed method handles the model uncertainty problem by optimizing the worst-case standard deviation value in the 1 -α interval $[y_{j,\sigma}^{L}(\mathbf{x}), y_{j,\sigma}^{U}(\mathbf{x})]$ instead of $\hat{y}_{j,\sigma}(\mathbf{x})$ used in MDF. This ensures that, in the worst case, the standard deviation of response y_2 does not exceed the upper specification limit. To sum up, the results in Fig. 6 indicate that all the solutions obtained by the proposed method meet the required specifications of the three responses.

5.5.3. Comparison of the obtained worst-case mean and standard deviation values considering model uncertainty

Similar to that in Section 5.4.3, the robust mean ($\hat{y}_{j,\mu}^{r}$, $j = 1, 2, 3$) and standard deviation ($\hat{y}_{j,\sigma}^{r}$, $j = 1, 2, 3$) values of the three responses obtained by the methods are shown in Fig. 7. The robust mean or standard deviation indicates the worst-case value in the 1- α confidence interval. According to Fig. 7a, the methods except for FDF2 obtain $\hat{y}_{j,\mu}^{r}$ values on the three responses that meet the required specifications. The solution of FDF2 fails to meet the required specification of response y_2 because the $\hat{y}_{2,\mu}^{r}$ value exceeds the upper specification limit $y_{2,\mu}^{\max} = 60.00$. According to Fig. 7b, except for the proposed method and FDF2 method, the compared methods fail to obtain solutions meeting the required standard deviation specifications. The $\hat{y}_{j,\sigma}^{r}$ values of the solutions of TDF, FDF1, RDF, and RFDF exceed the required upper specification limits $y_{j,\sigma}^{\max}$ on at least one response, and the $\hat{y}_{j,\sigma}^{r}$ values of a portion of the solutions of MDF violate the required specification limits $y_{j,\sigma}^{\max}$. Overall, the results in Fig. 7 indicate that either $\hat{y}_{j,\mu}^{r}$ or $\hat{y}_{j,\sigma}^{r}$ of the benchmark methods fails to meet the required specifications. In comparison, all the $\hat{y}_{j,\mu}^{r}$ and $\hat{y}_{j,\sigma}^{r}$ values of the proposed method are within the required specification limits. This shows the effectiveness of the proposed method.

To sum up, the optimization results of the two examples in Sections 5.4 and 5.5 have shown that the proposed MRO model is effective. The proposed model considers both the location and dispersion effects of multiple responses. Meanwhile, the uncertainty of the fitted regression models is considered. Thus, the solutions yielded by the proposed model can meet all the required specifications. In comparison, the models of the benchmark methods do not comprehensively consider the two effects and model uncertainty. Therefore, these benchmark methods may obtain solutions that fail to meet some specifications of the responses.

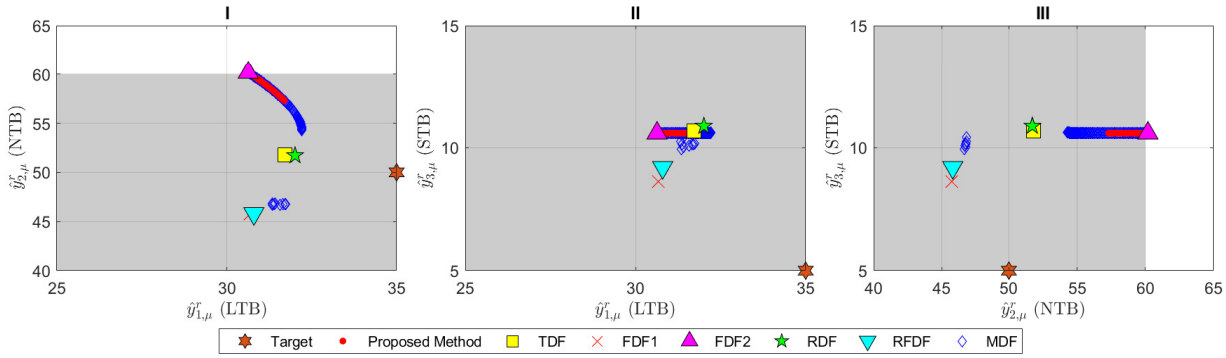

(a) Mean.

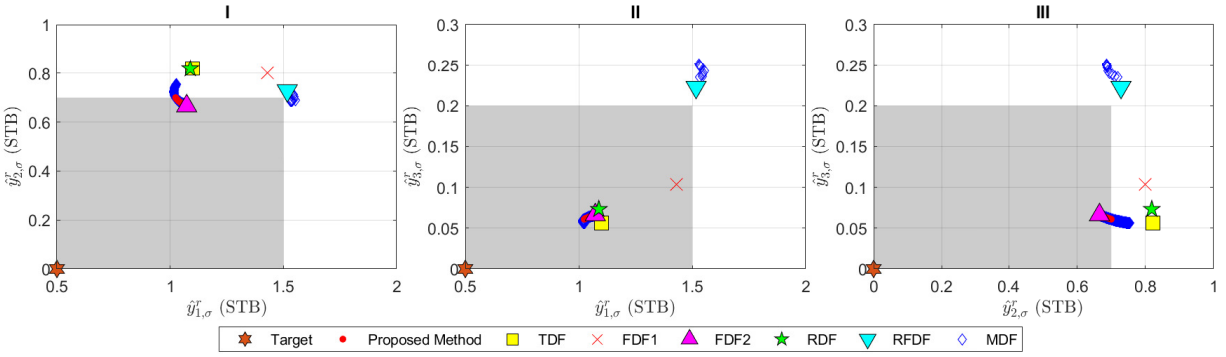

(b) Standard deviation.

Figure 7: Comparison of the robust mean ($\hat{y}^r_{j,\mu}$, $j = 1, 2, 3$) and standard deviation ($\hat{y}^r_{j,\sigma}$, $j = 1, 2, 3$) values of the 3 responses for the solutions obtained by the MRO methods in the synthetic example. The x-axis/y-axis in subfigures (a)-I, (a)-II, and (b)-III are $\hat{y}^r_{1,\mu}/\hat{y}^r_{2,\mu}$, $\hat{y}^r_{1,\mu}/\hat{y}^r_{3,\mu}$, and $\hat{y}^r_{2,\mu}/\hat{y}^r_{3,\mu}$. The x-axis/y-axis in subfigures (b)-I, (b)-II, and (b)-III are $\hat{y}^r_{1,\sigma}/\hat{y}^r_{2,\sigma}$, $\hat{y}^r_{1,\sigma}/\hat{y}^r_{3,\sigma}$, and $\hat{y}^r_{2,\mu}/\hat{y}^r_{3,\sigma}$. The areas that meet the required specifications are marked in gray.

5.6. Selecting the best compromise solution

The proposed method, a multi-objective MRO method, returns a set of non-dominated solutions with different desirability values on the location and dispersion effects. One merit of this multi-objective method is that DMs can further select the best compromise solution from the returned candidate solutions by investigating the trade-off between the two effects. In this selection procedure, DMs' preferences can be considered. The multi-objective decision methods, such as IPM (Li et al., 2016), TOPSIS (Lai et al., 1994; Ouyang et al., 2021) and the posterior preference articulation approach (Lee et al., 2018), can also be involved in this procedure to help DMs make a choice.

In this paper, we propose to use IPM to select the best compromise solution from the non-dominated solutions found by the proposed method. IPM has shown to be a simple and effective multi-objective decision method that is able to select the best compromise solution from the non-dominated solutions. IPM first defines an ideal point in the objective space and then selects the solution closest to the ideal point as the best compromise solution. Li et al. (2016) applied IPM to select the best compromise solution for

a key quality characteristic selection problem using NSGA-II. In this application, the ideas of solving the incommensurable problem of different objective functions and defining the ideal point using the information of the found non-dominated solutions are used. Let $L_{ns} = \{\mathbf{x}_1, ..., \mathbf{x}_s\}$ be the set of non-dominated solutions found by a multi-objective optimization algorithm and $f_j(\mathbf{x}_k)$ $(j = 1, ..., m$ and $k = 1, ..., s)$ be the jth objective function value for $\mathbf{x}_k$. The procedure of IPM used by Li et al. (2016) can be simply described as follows:

First, to solve the incommensurable problem, the normalized objective function value for each solution in L_{ns} is obtained by the Z-score normalization method as

$$f_j^N(\mathbf{x}_k) = \frac{f_j(\mathbf{x}_k) - \overline{f_j}}{\sigma(f_j)}, j = 1, ..., m, k = 1, ..., s, \tag{36}$$

where $\overline{f_j}$ and $\sigma(f_j)$ denote the mean and standard deviation of the objective function values of the solutions in L_{ns}, respectively.

Second, the ideal point is defined based on the normalized objective function values as

$$(f_1^*, ..., f_m^*) = \left(\min_{k \in \{1,...,s\}} f_1^N(\mathbf{x}_k), ..., \min_{k \in \{1,...,s\}} f_m^N(\mathbf{x}_k) \right). \tag{37}$$

Finally, by selecting the solution in L_{ns} that is closest to the ideal point, we obtain the best compromise solution as

$$\mathbf{x}^* = \arg\min_{\mathbf{x}_k \in L_{ns}} \sqrt{\sum_{j=1}^{m} (f_j^N(\mathbf{x}_k) - f_j^*)^2}. \tag{38}$$

We use the above mentioned IPM procedure to select the best compromise solution from the non-dominated solutions found by the proposed method. For a comparison purpose, the best compromise solution for the MDF method is also selected by IPM. The comparison of the search results between the benchmark methods and the proposed method with IPM in the CGA and synthetic examples are shown in Table 5, where the best solution $\mathbf{x}^* = (x_1^*, x_2^*, x_3^*)$, the predicted mean $\hat{y}_{j,\mu}(\mathbf{x}^*)$ and standard deviation $\hat{y}_{j,\sigma}(\mathbf{x}^*)$ on each response y_j $(j = 1, 2, 3)$, and the $1 - \alpha$ confidence limits $(y_{j,\sigma}^L(\mathbf{x}^*), y_{j,\sigma}^U(\mathbf{x}^*))$ and $(y_{j,\sigma}^L(\mathbf{x}^*), y_{j,\sigma}^U(\mathbf{x}^*))$ corresponding to each predicted mean and standard deviation are listed for each method.

According to Table 5, we find that, except for the proposed method, the predicted "mean/standard deviation" value or the upper/lower confidence limit of the solution found by the rest methods exceeds the required specification in the two examples. Specifically, in the CGA example, the $\hat{y}_{3,\sigma}(\mathbf{x}^*)$ values and the corresponding upper confidence limits $y_{3,\sigma}^U(\mathbf{x}^*)$ of TDF, FDF1, and RDF exceed the upper specification limit $y_{3,\sigma}^{\max} = 3.00$, and the upper confidence limits $y_{3,\sigma}^U(\mathbf{x}^*)$ of FDF2, RFDF, and MDF (with IPM) exceed the specification $y_{3,\sigma}^{\max} = 3.00$. In the synthetic example, the $\hat{y}_{2,\sigma}(\mathbf{x}^*)$ values and corresponding upper confidence limits $y_{2,\sigma}^U(\mathbf{x}^*)$ of TDF, FDF1, and RDF exceed the upper specification limit $y_{2,\sigma}^{\max} = 0.70$, the upper

Table 5: Comparison of the optimization results between the benchmark methods and the proposed method with IPM.

Example	Metric	The proposed method with IPM	TDF	FDF1	FDF2	RDF	RFDF	MDF with IPM
CGA	x_1^*	-0.415	-0.948	-0.567	-0.352	-0.817	-0.580	-0.624
	x_2^*	-0.167	-1.000	-0.938	-0.514	-0.826	-0.771	-0.450
	x_3^*	-1.000	-1.000	-1.000	-1.000	-0.887	-1.000	-1.000
	$\hat{y}_{1,\mu}(\mathbf{x}^*)$	4.691	4.717	5.078	4.952	4.712	4.924	4.651
	$\hat{y}_{2,\mu}(\mathbf{x}^*)$	0.323	0.256	0.340	0.356	0.290	0.327	0.299
	$\hat{y}_{3,\mu}(\mathbf{x}^*)$	26.567	25.260	25.561	26.278	26.044	25.897	26.351
	$\hat{y}_{1,\sigma}(\mathbf{x}^*)$	0.074	0.053	0.027	0.052	0.039	0.038	0.061
	$\hat{y}_{2,\sigma}(\mathbf{x}^*)$	0.047	0.059	0.055	0.050	0.051	0.054	0.051
	$\hat{y}_{3,\sigma}(\mathbf{x}^*)$	1.620	4.463	3.608	2.002	4.086	2.999	2.201
	$(y_{1,\mu}^L(\mathbf{x}^*), y_{1,\mu}^U(\mathbf{x}^*))$	(4.541,4.842)	(4.501,4.933)	(4.903,5.254)	(4.810,5.095)	(4.541,4.883)	(4.770,5.077)	(4.501,4.802)
	$(y_{2,\mu}^L(\mathbf{x}^*), y_{2,\mu}^U(\mathbf{x}^*))$	(0.273,0.374)	(0.203,0.309)	(0.287,0.394)	(0.303,0.409)	(0.245,0.335)	(0.276,0.379)	(0.251,0.346)
	$(y_{3,\mu}^L(\mathbf{x}^*), y_{3,\mu}^U(\mathbf{x}^*))$	(25.867,27.267)	(24.505,26.016)	(24.892,26.231)	(25.633,26.922)	(25.419,26.669)	(25.273,26.520)	(25.678,27.024)
	$(y_{1,\sigma}^L(\mathbf{x}^*), y_{1,\sigma}^U(\mathbf{x}^*))$	(-0.013,0.161)	(-0.053,0.159)	(-0.077,0.130)	(-0.043,0.147)	(-0.046,0.124)	(-0.059,0.135)	(-0.025,0.146)
	$(y_{2,\sigma}^L(\mathbf{x}^*), y_{2,\sigma}^U(\mathbf{x}^*))$	(0.029,0.066)	(0.029,0.088)	(0.029,0.081)	(0.030,0.070)	(0.026,0.075)	(0.030,0.078)	(0.030,0.073)
	$(y_{3,\sigma}^L(\mathbf{x}^*), y_{3,\sigma}^U(\mathbf{x}^*))$	(0.434,2.807)	(2.847,6.080)	(2.345,4.872)	(0.924,3.080)	(2.798,5.375)	(1.819,4.180)	(0.983,3.419)
Synthetic	x_1^*	-1.000	-1.000	1.000	-1.000	-0.884	1.000	-1.000
	x_2^*	-1.000	-1.000	0.941	-1.000	-1.000	-0.153	-1.000
	x_3^*	0.846	-0.163	-0.630	1.000	-0.114	-0.659	0.521
	$\hat{y}_{1,\mu}(\mathbf{x}^*)$	32.322	32.895	31.663	31.720	33.170	31.765	33.147
	$\hat{y}_{2,\mu}(\mathbf{x}^*)$	56.643	50.000	47.457	58.050	50.000	47.546	54.014
	$\hat{y}_{3,\mu}(\mathbf{x}^*)$	10.262	10.435	8.337	10.236	10.643	8.875	10.318
	$\hat{y}_{1,\sigma}(\mathbf{x}^*)$	0.959	1.012	1.356	0.984	1.001	1.451	0.935
	$\hat{y}_{2,\sigma}(\mathbf{x}^*)$	0.619	0.769	0.742	0.597	0.771	0.677	0.668
	$\hat{y}_{3,\sigma}(\mathbf{x}^*)$	0.012	0.015	0.058	0.012	0.036	0.184	0.013
	$(y_{1,\mu}^L(\mathbf{x}^*), y_{1,\mu}^U(\mathbf{x}^*))$	(31.296,33.349)	(31.715,34.074)	(30.672,32.654)	(30.633,32.806)	(32.010,34.330)	(30.798,32.732)	(32.067,34.227)
	$(y_{2,\mu}^L(\mathbf{x}^*), y_{2,\mu}^U(\mathbf{x}^*))$	(54.766,58.521)	(48.220,51.781)	(45.731,49.183)	(55.915,60.185)	(48.281,51.719)	(45.812,49.281)	(52.298,55.730)
	$(y_{3,\mu}^L(\mathbf{x}^*), y_{3,\mu}^U(\mathbf{x}^*))$	(9.930,10.595)	(10.181,10.690)	(8.053,8.622)	(9.877,10.595)	(10.399,10.888)	(8.549,9.202)	(10.033,10.603)
	$(y_{1,\sigma}^L(\mathbf{x}^*), y_{1,\sigma}^U(\mathbf{x}^*))$	(0.878,1.040)	(0.924,1.099)	(1.283,1.430)	(0.894,1.073)	(0.913,1.089)	(1.385,1.517)	(0.854,1.016)
	$(y_{2,\sigma}^L(\mathbf{x}^*), y_{2,\sigma}^U(\mathbf{x}^*))$	(0.555,0.684)	(0.717,0.822)	(0.683,0.800)	(0.528,0.666)	(0.723,0.819)	(0.624,0.729)	(0.611,0.725)
	$(y_{3,\sigma}^L(\mathbf{x}^*), y_{3,\sigma}^U(\mathbf{x}^*))$	(-0.038,0.063)	(-0.026,0.057)	(0.012,0.103)	(-0.042,0.066)	(-0.001,0.073)	(0.145,0.223)	(-0.031,0.058)

"____" denotes the mean or standard deviation is out of the required specification.

confidence limits $y_{1,\sigma}^U(\mathbf{x}^*)$, $y_{2,\sigma}^U(\mathbf{x}^*)$, and $y_{3,\sigma}^U(\mathbf{x}^*)$ of RFDF exceed the corresponding upper specification limits $y_{1,\sigma}^{\max} = 1.50$, $y_{2,\sigma}^{\max} = 0.70$, and $y_{3,\sigma}^{\max} = 0.20$, the upper confidence limit $y_{2,\mu}^U(\mathbf{x}^*)$ of FDF2 exceeds the upper specification limit $y_{2,\mu}^{\max} = 60.00$, and the upper confidence limit $y_{2,\sigma}^U(\mathbf{x}^*)$ of MDF (with IPM) exceeds the upper specification limit $y_{2,\sigma}^{\max} = 0.70$. These results show that the proposed method outperforms these benchmark methods.

5.7. Discussion

In an MRO problem, both the mean (location effect) and standard deviation (dispersion effect) of each response should be optimized in order to obtain a solution of high and stable performance. The necessity of considering the dispersion effect has been shown in the above two examples. The methods (i.e., TDF, FDF1, and RDF) considering only the location effect can obtain solutions that meet the "mean" specifications, while the obtained solutions of them fail to meet the "standard deviation" specifications. This means that the obtained solutions of these methods can obtain responses with high performance (i.e., the mean values of responses are close to the targets), but the performance of the responses may not be stable (i.e., the standard deviation of a response is great). From the point of view of robust design, the solutions from these methods are not robust enough. In comparison, the other four methods (i.e., the proposed method, FDF2, RFDF, and MDF) that consider both the location and dispersion effects can obtain solutions that meet all the "mean" and "standard deviation" specifications (without considering the uncertainty of the

fitted models). The solutions of these four methods are more robust than those of TDF, FDF1, and RDF. Moreover, the proposed method, FDF2, RFDF, and MDF provide three strategies to handle the dispersion effect with the optimization model. FDF2 uses a "max-min" scheme that maximizes the minimum degree of satisfaction with respect to the means and standard deviations of multiple responses. In this scheme, the objective function value of the optimization model is decided by a response's mean or standard deviation with the lowest desirability value, and thus the desirability values on other responses are neglected in the optimization model (Kim & Lin, 2006). RFDF treats the location effect of each response as a constraint in the optimization model. The degree of satisfaction of the overall location effect of multiple responses is set as the objective to be optimized. The RFDF method assumes that optimizing the location effect is more important than optimizing the dispersion effect. However, this assumption does not always hold in practice. In comparison, the proposed method and MDF use a more straightforward strategy that explicitly treats location and dispersion effects as two separate objectives to be optimized, and the multi-objective optimization models are constructed as simultaneously optimizing the overall desirability values of the two effects.

In MRO, the optimization for multiple responses is based on the fitted regression models with the data collected from experiments. In practice, we cannot obtain a perfectly fitted model that precisely predicts the true response value of given input variables, which is referred to as the model uncertainty problem. To obtain a reliable solution, model uncertainty cannot be neglected. The proposed method adopts a worst-case strategy as used by He et al. (2012) to handle model uncertainty. Specifically, this strategy constructs a robust desirability function that considers the worst response values in the confidence intervals of the responses predicted by the fitted models. This strategy can address the issue that over-optimistic but not reliable solutions are obtained. In the above examples, the proposed method, RDF, and RFDF have adopted this worst-case strategy to handle model uncertainty. However, it should be noted that RDF and RFDF only consider the uncertainty of the fitted "mean" regression models. As a result, the obtained solutions of RDF and RFDF fail to meet the "standard deviation" specifications on some responses in the two examples. In comparison, the proposed method considers the uncertainty of both the fitted "mean" and "standard deviation" models, and the obtained solutions meet all the required specifications.

The proposed method and MDF are based on the multi-objective optimization scheme, while other methods are based on the single objective optimization scheme. The multi-objective scheme can find a set of non-dominated solutions with different satisfactory levels on the location and dispersion effects by simultaneously optimizing the two effects. DMs can further select the best compromise solution by considering the trade-off between the two effects. In this selection step, DMs' preferences can be involved. For the single objective scheme, DMs need to consider the weights of location and dispersion effects in a very early phase of the MRO task when constructing the optimization model. However, DMs may lack enough domain knowledge to properly decide the weights of the two effects. In comparison, the multi-objective scheme does

not pre-allocate the weights for the two effects before the optimization. It simultaneously optimizes the two effects to obtain a set of non-dominated solutions that meet the specifications. Then, DMs can select the most desirable solution from these candidate solutions based on their preferences. The DMs can also re-select the best compromise solution when their preferences change without building and optimizing the model again. This shows the advantage of the multi-objective scheme. Furthermore, the multi-objective decision methods can help in the selection of the best compromise solution. In this paper, we propose to use IPM to select the solution closest to the defined ideal point as the best compromise solution. It is worth noting that, in the practical use of IPM, DMs can flexibly define the ideal point based on their preferences to obtain the final best compromise solution.

6. Evaluating the performance of the proposed NSGAII-DMS algorithm

The optimization results of the two test examples in Section 5 have shown that the constructed multi-objective MRO model is effective. In the proposed MRO method, the constructed multi-objective MRO model is optimized by a novel multi-objective optimization algorithm NSGAII-DMS. In this section, we further verify the search performance of NSGAII-DMS[1] with more experiments. The experimental design and the comparison of the search results between NSGAII-DMS and benchmark multi-objective optimization algorithms are given in Sections 6.1 and 6.2.

6.1. Experimental design

To show the effectiveness of NSGAII-DMS, four well-known multi-objective optimization algorithms including NSGA-II (Deb et al., 2002), SPEA2 (Zitzler et al., 2001), MOEA/D (the Tchebycheff approach version) (Zhang & Li, 2007), and DMS (Custódio et al., 2011) are used as benchmark algorithms. NSGA-II, SPEA2, and MOEA/D are three popular MOEAs. DMS is a multi-objective optimization algorithm based on the direct search. In NSGA-II, SPEA2, and MOEA/D, the population size and the maximum number of generations are set as 100 and 250, which yields the same number of function evaluations as NSGAII-DMS. The crossover probability and mutation probability are set as 0.9 and $1/n$, which are the same as NSGAII-DMS. In DMS, the same maximum number of function evaluations (i.e., 25,000) as NSGAII-DMS is used. Moreover, as suggested by Custódio et al. (2011), the initial value of the step size parameter is set as $\alpha_0 = 1$, and the step size is halved at failure iterations and is maintained at successful iterations in DMS. Since the benchmark algorithms and NSGAII-DMS are stochastic optimization algorithms, the experiments applying these methods to solve the CGA and synthetic MRO problems described in Section 5.1 are repeated 30 times with different running seeds. The results of the 30 experimental runs are used to compare the performance of these methods. All these optimization algorithms are implemented in Matlab

[1]The source code of NSGAII-DMS is available at https://github.com/andali89/nsgaii_dms.

R2021a and the experiments are conducted on a PC with 16 GB RAM and a 3.6 GHz CPU. We adopt three performance metrics, i.e., hypervolume (HV) (Yuan et al., 2016), the inverted generational distance (IGD) (Li et al., 2020; Li & He, 2020), and the diversity metric (DME) (Deb et al., 2002), to evaluate the search performance. A brief introduction of these metrics is given below.

HV measures the hypervolume dominated by the non-dominated solutions of a multi-objective optimization algorithm in the objective space. A larger HV value denotes a better quality of the non-dominated solutions. Let L_{ns} be a set of non-dominated solutions and $\mathbf{r} = (r_1, r_2, ..., r_m)$ be a given reference point in the objective space. The hypervolume of L_{ns} with respect to $\mathbf{r}$ is obtained as

$$HV(L_{ns}) = volume\left(\bigcup_{\mathbf{x}\in L_{ns}} \prod_{j=1}^{m} |r_j - f_j(\mathbf{x})|\right), \tag{39}$$

where $f_j(\mathbf{x})$ denotes the value of the jth objective function obtained by $\mathbf{x}$.

IGD measures the similarity between the Pareto optimal solutions and the non-dominated solutions found by a multi-objective optimization algorithm. The lower the IGD value is, the better the performance of the optimization algorithm is. Let L_p be the set of Pareto optimal solutions and L_{ns} be a set of non-dominated solutions found by a multi-objective optimization algorithm. The IGD value of L_{ns} with respect to L_p is defined as

$$IGD(L_{ns}) = \frac{1}{|L_p|} \sum_{\mathbf{x}_p \in L_p} \min_{\mathbf{x}\in L_{ns}} D(\mathbf{x}_p, \mathbf{x}), \tag{40}$$

where $|L_p|$ denotes the number of solutions in L_p and $D(\mathbf{x}_p, \mathbf{x})$ denotes the Euclidean distance between solutions $\mathbf{x}_p$ and $\mathbf{x}$ in the objective space.

DME measures the spread degree of the non-dominated solutions found by a multi-objective optimization algorithm. A lower DME value denotes the found solutions spread more uniformly in the non-dominated front. Let L_{ns} be a set of non-dominated solutions. The DME value of L_{ns} is obtained as

$$DME(L_{ns}) = \frac{d_f + d_l + \sum_{i=1}^{|L_{ns}|-1} |d_i - \bar{d}|}{d_f + d_l + (|L_{ns}| - 1)\bar{d}} \tag{41}$$

where $|L_{ns}|$ denotes the number of the solutions in L_{ns}, $d_1, d_2, ..., d_{|L_{ns}|-1}$ are the Euclidean distances between the consecutive solutions in L_{ns} in the objective space, d_f and d_l are the Euclidean distances between the two extreme solutions and their neighbor solutions in the objective space, and $\bar{d}$ is the average of $d_1, d_2, ..., d_{|L_{ns}|-1}$.

The ranges of different objective functions can be very different. Thus, we first normalize each objective function value based on the max-min normalization method, where the maximum and minimum values are obtained based on the union of the solutions found by all the compared optimization algorithms. The HV, IGD, and DME values for each algorithm are then calculated based on the normalized objective function

values. To compute the HV value, the reference point $\mathbf{r} = (r_1, r_2, ..., r_m)$ should be given. We define each element of the reference point as $r_j = 1.1$, $j = 1, 2, ..., m$ as suggested by Yuan et al. (2016). To calculate the IGD value, we need to know the true Pareto front of the problem. In this paper, we obtain the non-dominated front based on the solutions found by all the compared methods on the 30 runs and let this non-dominated front be the approximate Pareto front for the calculation of IGD as suggested by Li et al. (2020). For a more detailed description of the calculation for the three metrics, please refer to Li et al. (2020).

6.2. Comparison of the search performance

Table 6 shows the results of the three performance metrics and the computation time (CPU time) obtained by the optimization algorithms on the two examples. In the table, the mean and standard deviation values on each performance metric are shown for each method. Each "P-value" column shows the statistical significance test results comparing NSGAII-DMS with a benchmark method based on the Wilcoxon rank-sum test (Wilcoxon, 1945) with a significance level of 0.05.

Overall, for both the CGA and synthetic examples, NSGAII-DMS obtains better HV, IGD, and DME results than the benchmark algorithms. First, NSGAII-DMS obtains a significantly higher HV value than the benchmark algorithms in the two examples. This means that the non-dominated solutions obtained by NSGAII-DMS dominate a larger area than the benchmark algorithms in the objective space. Second, NSGAII-DMS obtains a significantly lower IGD value than the benchmark algorithms in the two examples. This shows that the non-dominated front obtained by NSGAII-DMS is more similar to the Pareto front than the benchmark algorithms. The IGD and HV results show that NSGAII-DMS obtains higher quality solutions than the benchmark algorithms. Finally, NSGAII-DMS obtains a significantly lower DME value than the benchmark algorithms in the two examples. This shows that the solutions obtained by NSGAII-DMS are distributed more uniformly in the non-dominated front than the solutions obtained by benchmark algorithms, which means that NSGAII-DMS has a better spread property than the benchmark algorithms.

Moreover, in the two examples, NSGAII-DMS requires slightly less computation time than NSGA-II, while requiring more computation time than SPEA2, MOEA/D, and DMS. This is because the non-dominated sorting approach used in NSGAII-DMS and NSGA-II requires more computation time than the solution sorting approaches in SPEA2, MOEA/D, and DMS. However, seeing that NSGAII-DMS can obtain better IGD, HV, and DME results than other algorithms and the computation time required by NSGAII-DMS are acceptable from a practical point of view, it is a better choice to use the proposed NSGAII-DMS instead of the benchmark algorithms.

The above results have shown that the proposed NSGAII-DMS outperforms the benchmark multi-objective optimization algorithms. The following reasons can explain the effectiveness of NSGAII-DMS:

Table 6: Comparison of the search performance between NSGAII-DMS and benchmark multi-objective optimization methods.

Example	Metric	NSGAII-DMS		NSGA-II			SPEA2			MOEA/D			DMS		
		Mean	Std.	Mean	Std.	P-value	Mean	Std.	P-value	Mean	Std.	P-value	Mean	Std.	P-value
CGA	HV	1.1002	0.0001	1.0988	0.0002	**0.0000***	1.0823	0.0087	**0.0000***	1.0853	0.0017	**0.0000***	1.0975	0.0005	**0.0000***
	IGD	0.0048	0.0005	0.0053	0.0002	**0.0001***	0.0285	0.0144	**0.0000***	0.0353	0.0027	**0.0000***	0.0081	0.0006	**0.0000***
	DME	0.2393	0.0176	0.4203	0.0267	**0.0000***	1.0691	0.0618	**0.0000***	0.8995	0.0180	**0.0000***	0.5994	0.0211	**0.0000***
	Time (S)	37.3	2.3	53.6	0.5	**0.0000***	18.9	0.5	**0.0000***	20.1	0.7	**0.0000***	18.5	0.9	**0.0000***
Synthetic	HV	1.1008	0.0000	1.0993	0.0029	**0.0000***	1.0929	0.0023	**0.0000***	1.0979	0.0004	**0.0000***	1.0997	0.0001	**0.0000***
	IGD	0.0052	0.0005	0.0068	0.0066	**0.0000***	0.0216	0.0073	**0.0000***	0.0216	0.0014	**0.0000***	0.0054	0.0002	**0.0017***
	DME	0.1864	0.0201	0.4456	0.0693	**0.0000***	1.1039	0.0716	**0.0000***	0.8669	0.0180	**0.0000***	0.3504	0.0198	**0.0000***
	Time (S)	34.9	2.3	53.1	0.9	**0.0000***	17.8	0.5	**0.0000***	20.3	1.3	**0.0000***	15.5	0.4	**0.0000***

- First, NSGA-II is a classical MOEA with a good global search capability. Thus, adopting the NSGA-II-based search mechanism during the early optimization stage makes NSGAII-DMS quickly find a set of high-quality non-dominated solutions, which lays a good foundation for the following DMS process.

- Second, DMS focuses on searching in the local space around the currently found non-dominated solutions and it has shown to have excellent convergence behaviors. Therefore, adopting the DMS-based search mechanism during the late optimization stage of NSGAIII-DMS is a good strategy to further tune the (relatively) good solutions found by the NSGA-II process.

- Finally, the DMS-based search mechanism adopted in NSGAII-DMS is not exactly the same as that in the traditional DMS algorithm. In the DMS process of NSGAII-DMS, the crowding distance measure is also used to guide selecting the poll center and rejecting superfluous solutions if the non-dominated set L_{ns} exceeds the maximum size. Since the crowding distance can effectively measure the crowding degree of each solution in the non-dominated front, the non-dominated solutions with a good spread property can be maintained by NSGAII-DMS.

7. Conclusions

In this paper, we propose a robust MRO method using a hybrid multi-objective optimization algorithm, i.e., NSGAII-DMS. Compared with the traditional single objective optimization based MRO methods, the proposed method can find a set of non-dominated solutions instead of one single solution. DMs can select the best compromise solution from the non-dominated solutions based on their preferences. The proposed method considers both the location and dispersion effects of multiple responses while considering model uncertainty. Based on the idea of the robust desirability function (He et al., 2012) that can address model uncertainty, we form two overall desirability functions to model the location and dispersion effects, respectively. Then, we construct the MRO model as a multi-objective optimization problem that simultaneously optimizes the two modeled overall desirability functions. To solve the model, we propose the NSGAII-DMS algorithm that combines the search mechanisms of NSGA-II and DMS. The optimization results of the two test examples show that the proposed model can obtain robust solutions with desirable location and dispersion effects results while ensuring the solutions' reliability by addressing model uncertainty. The

optimization results also show that IPM can be a good tool to help DMs select the best compromise solution from the non-dominated solutions found by NSGAII-DMS, as IPM can find a solution with a good balance between the location and dispersion effects. Further analyses illustrate that the NSGAII-DMS algorithm shows significantly better search performance than several well-known multi-objective optimization algorithms, including NSGA-II, SPEA2, MOEA/D, and DMS.

The proposed MRO model defines the location and dispersion effects as two optimization objectives. One advantage of this formulation is that DMs can further select the best compromise solution from the obtained non-dominated solutions considering the trade-off between the two effects. This formulation also has a good scalability property, since the increase in the number of responses does not change the form of the optimization model. However, the drawback of this formulation is that the trade-offs among multiple responses cannot be straightforwardly considered by the DMs when selecting the best compromise solution. Thus, one of our future research interests is to establish an MRO method that can provide DMs with more flexibility to consider the trade-offs among multiple responses for decision making. Moreover, being one desirability function based MRO method, the proposed method does not consider the correlations among responses. Hence, building a multi-objective optimization based MRO method that can handle the correlations among multiple responses is also worth studying in the future.

Appendix A. Tuning parameters for NSGAII-DMS

As we analyzed in Section 5.2, three parameters, including the maximum number of generations of the GA process T, the initial step size parameter α_0, and the parameter β, are required to be tuned for NSGAII-DMS. Therefore, in this section, we conduct the tuning experiments to find a desirable setting for the three parameters. In the experiments, we examine four values of T (i.e., $T \in \{50, 100, 150, 200\}$), examine five values of α_0 (i.e., $\alpha_0 \in \{0.2, 0.4, ..., 1\}$), and examine nine values of β (i.e., $\beta \in \{0.50, 0.55, ..., 0.90\}$). This results in a set $\{(T, \alpha_0, \beta) | T \in \{50, 100, 150, 200\}, \alpha_0 \in \{0.2, 0.4, ..., 1\}, \beta \in \{0.5, 0.55, ..., 0.90\}\}$ of 180 candidate parameter settings. The details of these parameter settings are shown in Table A.1.

In the experiments, we apply NSGAII-DMS with each parameter setting shown in Table A.1 to the CGA example to tune the parameters. The experiment runs 10 times for each parameter setting, which results in 10 sets of the non-dominated solutions. To evaluate the goodness of the obtained non-dominated solutions, the HV metric described in Section 6.1 is adopted. We can obtain 10 HV values for the 10 sets of non-dominated solutions. Considering both the mean and variance of the obtained HV values, we further transform the 10 HV values into Taguchi's signal-to-noise (S/N) ratio as suggested by Sadeghi et al. (2011). The S/N ratio is used as the final performance metric to evaluate the goodness of the solutions from each parameter setting. Since the HV metric is larger the better, the following formula is adopted to calculate

Table A.1: Parameter settings to be examined in the tuning experiments.

ID	T	α_0	β
1	50	0.2	0.50
2	50	0.2	0.55
	...		
9	50	0.2	0.90
10	50	0.4	0.50
11	50	0.4	0.55
	...		
45	50	1	0.90
46	100	0.2	0.50
47	100	0.2	0.55
	...		
180	200	1	0.90

the S/N ratio:

$$S/N \text{ ratio} = -10 \log \left(\frac{1}{10} \sum_{r=1}^{10} (\frac{1}{HV_r})^2 \right) \tag{A.1}$$

where HV_r denotes the HV value of the rth experimental run. A large S/N ratio usually denotes a high mean value and a small variance of the HV metric, which means the parameter setting obtains good search performance.

Fig. A.1 shows the S/N ratios of the parameter settings shown in Table A.1. According to the figure, the best S/N ratio is achieved when the 62th parameter setting (i.e., $T = 100$, $\alpha_0 = 0.4$, $\beta = 0.85$) is adopted. According to the tuning results of these parameters, the maximum number of generations of the GA process is set as $T = 100$, neither a too large nor a too small value. This indicates T should be set as a proper value to make both the GA process and the DMS process conduct enough iterations. Moreover, compared with the original DMS algorithm, which set $\alpha_0 = 1$ and $\beta = 0.5$, the tuning results indicate that NSGAII-DMS should use a smaller α_0 (i.e., 0.4) and a larger β (i.e. 0.85). This indicates that the initial search step is smaller and the step size reduces slower in the DMS process of NSGAII-DMS than in the original DMS algorithm. This is because we have already used the NSGA-II process for the global search in the early optimization stage of NSGAII-DMS. It would be good to set α_0 as a relatively small value to make the DMS focus on the local search. Moreover, a slightly large β (i.e., 0.85) also guarantees the search step does not shrink too fast.

Declarations of interest: none

References

Box, G. E., Draper, N. R. et al. (1987). *Empirical model-building and response surfaces* volume 424. Wiley New York.

Chapman, J. L., Lu, L., & Anderson-Cook, C. M. (2014a). Incorporating response variability and estimation uncertainty into pareto front optimization. *Computers & Industrial Engineering*, *76*, 253 – 267.

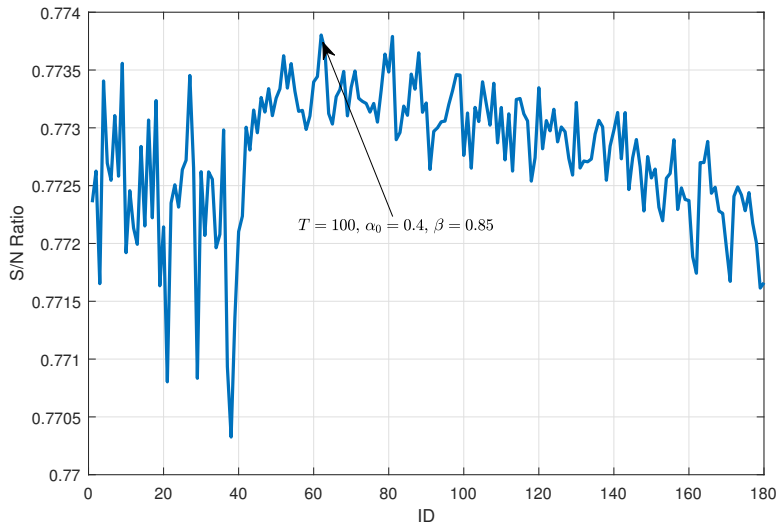

Figure A.1: The S/N ratios of different parameter settings.

Chapman, J. L., Lu, L., & Anderson-Cook, C. M. (2014b). Process optimization for multiple responses utilizing the Pareto front approach. *Quality Engineering*, *26*(3), 253–268.

Costa, N., & Lourenço, J. (2017). Reproducibility of nondominated solutions. *Chemometrics and Intelligent Laboratory Systems*, *168*, 1 – 9.

Costa, N., Lourenço, J., & Pereira, Z. L. (2012a). Responses modeling and optimization criteria impact on the optimization of multiple quality characteristics. *Computers & Industrial Engineering*, *62*(4), 927 – 935.

Costa, N. R., Lourenço, J., & Pereira, Z. L. (2012b). Multiresponse optimization and Pareto frontiers. *Quality and Reliability Engineering International*, *28*(7), 701–712.

Custódio, A. L., Madeira, J. F. A., Vaz, A. I. F., & Vicente, L. N. (2011). Direct multisearch for multiobjective optimization. *SIAM Journal on Optimization*, *21*(3), 1109–1140.

Deb, K., Agrawal, S., Pratap, A., & Meyarivan, T. (2002). A fast and elitist multiobjective genetic algorithm: NSGA-II. *IEEE Transactions on Evolutionary Computation*, *6*(2), 182–197.

Derringer, G. C. (1994). A balancing act: optimizing a products properties. *Quality Progress*, *27*(6), 51–58.

Feng, Z., Wang, J., Ma, Y., & Tu, Y. (2021). Robust parameter design based on gaussian process with model uncertainty. *International Journal of Production Research*, *59*(9), 2772–2788.

Gülpınar, N., & Rustem, B. (2007). Robust optimal decisions with imprecise forecasts. *Computational Statistics & Data Analysis*, *51*(7), 3595 – 3611.

He, Y., He, Z., Lee, D.-H., Kim, K.-J., Zhang, L., & Yang, X. (2017). Robust fuzzy programming method for MRO problems considering location effect, dispersion effect and model uncertainty. *Computers & Industrial Engineering*, *105*, 76 – 83.

He, Z., Zhu, P.-F., & Park, S.-H. (2012). A robust desirability function method for multi-response surface optimization considering model uncertainty. *European Journal of Operational Research*, *221*(1), 241–247.

Jauregi, P., Gilmour, S., & Varley, J. (1997). Characterisation of colloidal gas aphrons for subsequent use for protein recovery. *Chemical Engineering Journal*, *65*(1), 1 – 11.

Kazemzadeh, R. B., Bashiri, M., Atkinson, A. C., & Noorossana, R. (2008). A general framework for multiresponse optimization problems based on goal programming. *European Journal of Operational Research*, *189*(2), 421 – 429.

Khuri, A. I., & Conlon, M. (1981). Simultaneous optimization of multiple responses represented by polynomial regression

functions. *Technometrics*, *23*(4), 363–375.

Kim, K.-J., & Lin, D. K. (2006). Optimization of multiple responses considering both location and dispersion effects. *European Journal of Operational Research*, *169*(1), 133 – 145.

Kim, K.-J., & Lin, D. K. J. (1998). Dual response surface optimization: A fuzzy modeling approach. *Journal of Quality Technology*, *30*(1), 1–10.

Kim, K.-J., & Lin, D. K. J. (2000). Simultaneous optimization of mechanical properties of steel by maximizing exponential desirability functions. *Journal of the Royal Statistical Society: Series C (Applied Statistics)*, *49*(3), 311–325.

Ko, Y.-H., Kim, K.-J., & Jun, C.-H. (2005). A new loss function-based method for multiresponse optimization. *Journal of Quality Technology*, *37*(1), 50–59.

Köksoy, O., & Doganaksoy, N. (2003). Joint optimization of mean and standard deviation using response surface methods. *Journal of Quality Technology*, *35*(3), 239–252.

Köksoy, O., & Yalcinoz, T. (2008). Robust design using Pareto type optimization: A genetic algorithm with arithmetic crossover. *Computers & Industrial Engineering*, *55*(1), 208 – 218.

Lai, Y.-J., Liu, T.-Y., & Hwang, C.-L. (1994). TOPSIS for MODM. *European Journal of Operational Research*, *76*(3), 486 – 500.

Lee, D.-H., Jeong, I.-J., & Kim, K.-J. (2009). A posterior preference articulation approach to dual-response-surface optimization. *IIE Transactions*, *42*(2), 161–171.

Lee, D.-H., Jeong, I.-J., & Kim, K.-J. (2018). A desirability function method for optimizing mean and variability of multiple responses using a posterior preference articulation approach. *Quality and Reliability Engineering International*, *34*(3), 360–376.

Lee, D.-H., Kim, K.-J., & Köksalan, M. (2011). A posterior preference articulation approach to multiresponse surface optimization. *European Journal of Operational Research*, *210*(2), 301 – 309.

Li, A.-D., & He, Z. (2020). Multiobjective feature selection for key quality characteristic identification in production processes using a nondominated-sorting-based whale optimization algorithm. *Computers & Industrial Engineering*, *149*, 106852.

Li, A.-D., He, Z., & Zhang, Y. (2016). Bi-objective variable selection for key quality characteristics selection based on a modified NSGA-II and the ideal point method. *Computers in Industry*, *82*, 95 – 103.

Li, A.-D., Xue, B., & Zhang, M. (2020). Multi-objective feature selection using hybridization of a genetic algorithm and direct multisearch for key quality characteristic selection. *Information Sciences*, *523*, 245 – 265.

Luo, B., Zheng, J., Xie, J., & Wu, J. (2008). Dynamic crowding distance?a new diversity maintenance strategy for moeas. In *2008 Fourth International Conference on Natural Computation* (pp. 580–585). volume 1.

Montgomery, D. C. (2017). *Design and analysis of experiments*. John wiley & sons.

Myers, R. H. (1999). Response surface methodology—current status and future directions. *Journal of Quality Technology*, *31*(1), 30–44.

Myers, R. H., Montgomery, D. C., & Anderson-Cook, C. M. (2016). *Response surface methodology: process and product optimization using designed experiments*. John Wiley & Sons.

Oh, I., Lee, J., & Moon, B. R. (2004). Hybrid genetic algorithms for feature selection. *IEEE Transactions on Pattern Analysis and Machine Intelligence*, *26*(11), 1424–1437.

Ouyang, L., Chen, J., Ma, Y., Park, C., & Jin, J. J. (2020). Bayesian closed-loop robust process design considering model uncertainty and data quality. *IISE Transactions*, *52*(3), 288–300.

Ouyang, L., Ma, Y., Wang, J., & Tu, Y. (2017). A new loss function for multi-response optimization with model parameter uncertainty and implementation errors. *European Journal of Operational Research*, *258*(2), 552 – 563.

Ouyang, L., Park, C., Ma, Y., Ma, Y., & Wang, M. (2021). Bayesian hierarchical modelling for process optimisation. *International Journal of Production Research*, *59*(15), 4649–4669.

Ouyang, L., Zhu, S., Ye, K., Park, C., & Wang, M. (2022). Robust bayesian hierarchical modeling and inference using scale mixtures of normal distributions. *IISE Transactions*, *54*(7), 659–671.

Peterson, J. J., Miró-Quesada, G., & del Castillo, E. (2009). A bayesian reliability approach to multiple response optimization with seemingly unrelated regression models. *Quality Technology & Quantitative Management*, *6*(4), 353–369.

Pignatiello, J. J., Jr (1993). Strategies for robust multiresponse quality engineering. *IIE Transactions*, *25*(3), 5–15.

Sadeghi, A., Alem-Tabriz, A., & Zandieh, M. (2011). Product portfolio planning: a metaheuristic-based simulated annealing algorithm. *International Journal of Production Research*, *49*(8), 2327–2350.

Shin, S., & Cho, B. R. (2009). Studies on a biobjective robust design optimization problem. *IIE Transactions*, *41*(11), 957–968.

Taguchi, G. (1986). *Introduction to quality engineering: designing quality into products and processes*. New York: Asian Productivity Organization, UNIPUB/Kraus Internationl White Plains.

Vining, G. G., & Myers, R. H. (1990). Combining Taguchi and response surface philosophies: A dual response approach. *Journal of Quality Technology*, *22*(1), 38–45.

Wang, J., Ma, Y., Ouyang, L., & Tu, Y. (2016). A new bayesian approach to multi-response surface optimization integrating loss function with posterior probability. *European Journal of Operational Research*, *249*(1), 231 – 237.

Wang, J., Ma, Y., Ouyang, L., & Tu, Y. (2020). Bayesian modeling and optimization for multi-response surfaces. *Computers & Industrial Engineering*, *142*, 106357.

Wilcoxon, F. (1945). Individual comparisons by ranking methods. *Biometrics Bulletin*, *1*(6), 80 – 83.

Xu, D., & Albin, S. L. (2003). Robust optimization of experimentally derived objective functions. *IIE Transactions*, *35*(9), 793–802.

Yang, S., Wang, J., & Tu, Y. (2021). Bayesian robust parameter design for ordered response. *International Journal of Production Research*, *0*(0), 1–21. doi:10.1080/00207543.2021.1930235.

Yuan, Y., Xu, H., Wang, B., & Yao, X. (2016). A new dominance relation-based evolutionary algorithm for many-objective optimization. *IEEE Transactions on Evolutionary Computation*, *20*(1), 16–37.

Zeybek, M., Köksoy, O., & Robinson, T. J. (2020). A dual-response surface modeling approach for gamma robust design. *Quality and Reliability Engineering International*, *36*(1), 315–327.

Zhang, Q., & Li, H. (2007). MOEA/D: A multiobjective evolutionary algorithm based on decomposition. *IEEE Transactions on Evolutionary Computation*, *11*(6), 712–731.

Zitzler, E., Laumanns, M., & Thiele, L. (2001). SPEA2: Improving the strength pareto evolutionary algorithm. In *Evolutionary Methods for Design, Optimization and Control with Applications to Industrial Problems. Proceedings of the EUROGEN'2001. Athens. Greece, September 19-21* (pp. 95–100).